Article

Current Biology

Intracranial Recordings Reveal Unique Shape and Timing of Responses in Human Visual Cortex during Illusory Visual Events

Highlights

- Stimulus changes elicit a hierarchical processing cascade in visual regions
- Perceptual changes during binocular rivalry elicit a reversed-hierarchy cascade
- Responses during binocular rivalry rise characteristically slowly
- Top-down signals may serve to stabilize a new percept during binocular rivalry

Authors

Maartje C. de Jong, Mariska J. Vansteensel, Raymond van Ee, ..., H. Chris Dijkerman, Serge O. Dumoulin, Tomas Knapen

Correspondence

m.dejong@spinozacentre.nl

In Brief

de Jong et al. find that the processing hierarchy of perceptual changes during binocular rivalry is reversed compared to processing of stimulus changes. Binocular rivalry responses in ventral regions precede those in early visual regions. They speculate top-down signals stabilize a new perceptual interpretation of a binocular rivalry stimulus.

de Jong et al., 2020, Current Biology *30*, 1–12
August 17, 2020
https://doi.org/10.1016/j.cub.2020.05.082

CellPress

Current Biology

CellPress

Article

Intracranial Recordings Reveal Unique Shape and Timing of Responses in Human Visual Cortex during Illusory Visual Events

Maartje C. de Jong,[1,2,9,*] Mariska J. Vansteensel,[3] Raymond van Ee,[4,5,6] Frans S.S. Leijten,[3] Nick F. Ramsey,[3] H. Chris Dijkerman,[7] Serge O. Dumoulin,[1,2,7,8] and Tomas Knapen[1,2,8]

[1]Spinoza Centre for Neuroimaging, Meibergdreef 47, 1105 Amsterdam, the Netherlands
[2]Experimental and Applied Psychology, VU University, Van der Boechorststraat 7, 1081 Amsterdam, the Netherlands
[3]UMC Utrecht Brain Center, Department of Neurology and Neurosurgery, University Medical Center Utrecht, Heidelberglaan 100, 3584 Utrecht, the Netherlands
[4]Department of Brain, Behavior & Cognition, Philips Research Laboratories, High Tech Campus 34, 5656 Eindhoven, the Netherlands
[5]Experimental Psychology, University of Leuven, Tiensestraat 102 - box 3711, Leuven 3000, Belgium
[6]Department of Biophysics, Donders Institute, Radboud University, PO Box 9010//066, 6500 Nijmegen, the Netherlands
[7]Experimental Psychology, Helmholtz Institute, Utrecht University, Heidelberglaan 1, 3584 Utrecht, the Netherlands
[8]These authors contributed equally
[9]Lead Contact
*Correspondence: m.dejong@spinozacentre.nl
https://doi.org/10.1016/j.cub.2020.05.082

SUMMARY

During binocular rivalry, perception spontaneously changes without any alteration to the visual stimulus. What neural events bring about this illusion that a constant stimulus is changing? We recorded from intracranial electrodes placed on the occipital and posterior temporal cortex of two patients with epilepsy while they experienced illusory changes of a face-house binocular-rivalry stimulus or observed a control stimulus that physically changed. We performed within-patient comparisons of broadband high-frequency responses, focusing on single epochs recorded along the ventral processing stream. We found transient face- and house-selective responses localized to the same electrodes for illusory and physical changes, but the temporal characteristics of these responses markedly differed. In comparison with physical changes, responses to illusory changes were longer lasting, in particular exhibiting a characteristic slow rise. Furthermore, the temporal order of responses across the visual hierarchy was reversed for illusory as compared to physical changes: for illusory changes, higher order fusiform and parahippocampal regions responded before lower order occipital regions. Our tentative interpretation of these findings is that two stages underlie the initiation of illusory changes: a destabilization stage in which activity associated with the impending change gradually accumulates across the visual hierarchy, ultimately graduating in a top-down cascade of activity that may stabilize the new perceptual interpretation of the stimulus.

INTRODUCTION

When your two eyes are each presented with a different image, you will experience an intriguing phenomenon known as binocular rivalry: instead of perceiving a blend of the two images, you alternatingly perceive either one or the other. These changes in perception occur even though the stimulus is constant. For over 150 years, there has been a debate in the literature how such illusory changes are initiated in the brain [1]. In the absence of any external event, which internal neural events give rise to a spontaneous change in conscious perception?

Illusory changes involve fluctuations in neural activity that track the alternations between perceptual states, very similar to when a stimulus physically changes back and forth between two different images. Using functional magnetic resonance imaging (fMRI) in humans and electrophysiology in monkeys, perception-driven response fluctuations have been reported for both illusory and physical changes in brain regions ranging from the lateral geniculate nucleus [2, 3] to occipital [4–8], temporal [9–13], parietal [14], and frontal cortex [15, 16]. This similarity in localization suggests that illusory and physical changes involve the same percept-selective neural networks. The fundamental difference in mechanism of initiation between illusory and physical changes is, apparently, not reflected in the localization of these networks but in other characteristics.

Here, we focus on the temporal characteristics of transient neural responses that occur at the moment of a perceptual change (rather than searching for sustained response fluctuations that reflect perceptual state) [17, 18]. Whereas physical changes elicit a bottom-up processing stream characterized by sequential activation of lower to higher order visually responsive regions [19, 20], endogenous initiation of illusory changes is thought to be a gradual process that requires coordination between different components of the visual hierarchy [21–26]. We

Please cite this article in press as: de Jong et al., Intracranial Recordings Reveal Unique Shape and Timing of Responses in Human Visual Cortex during Illusory Visual Events, Current Biology (2020), https://doi.org/10.1016/j.cub.2020.05.082

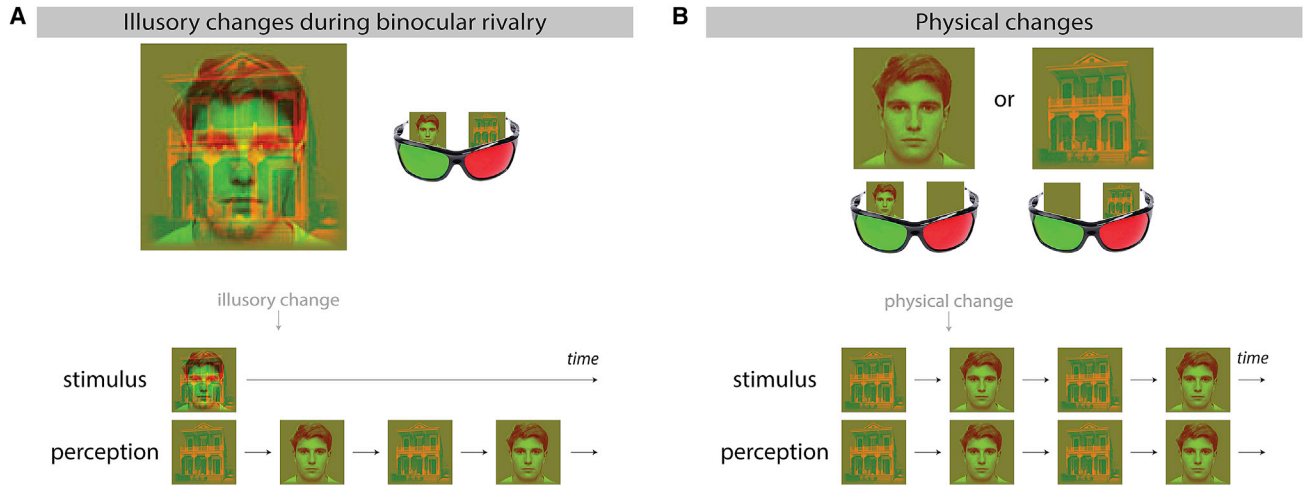

Figure 1. Stimuli

(A) Binocular rivalry stimulus. By means of red-green anaglyph glasses, a face image was presented to one eye and a house image to the other eye. Participants experienced illusory changes in the stimulus, i.e., perception changed while the stimulus was constant.

(B) Physical changes consisted of an on-screen change in the stimulus: the house image was replaced by the face image, or vice versa, and perception changed accordingly. Physical and illusory changes were similar in appearance but differed regarding their initiation: the former were initiated by on-screen changes, whereas the latter were spontaneously initiated in the participants' brain.

hypothesized that this coordination process results in a different temporal ordering of activations across different visual regions, contrasting the sequential lower to higher order activations for physical changes. In addition, we expected that a reverberating coordination process may result in a relatively slow and gradual buildup of percept-selective responses [25, 27]. To investigate these hypotheses, we analyzed the shape and timing of perception-selective neural responses at the single epoch level. Importantly, a single-epoch approach does not involve averaging across epochs aligned in time to behavioral reports. Thereby, it allows direct comparison of physical and illusory changes irrespective of their possible differences in reaction times, thus bypassing this long-standing problem in the study of binocular rivalry [27–29].

Our aim requires data that combine high spatial and temporal resolution with wide spatial coverage and high signal-to-noise ratio. Intracranial electro-encephalography meets these criteria, as this technique is superior to monkey electrophysiology with respect to spatial coverage, superior to fMRI with respect to temporal precision, and superior to scalp recordings with respect to signal-to-noise ratio and spatial precision, in particular regarding high-frequency oscillations [30, 31]. Previously described intracranial recordings in humans showed that responses in the medial temporal lobe reflect perception independent from modulations in visual input [10, 13, 32, 33]. Here, we analyzed intracranial recordings obtained from patients with epilepsy who had electrodes implanted directly on parts of the occipital and posterior temporal cortices for diagnostic purposes [34]. Human intracranial recordings that include occipital coverage (rather than medial temporal lobe) are rare and extremely valuable, as they can provide a bridge between electrophysiological studies in monkey visual cortex and non-invasive neuro-imaging studies in humans.

The patients experienced illusory changes of a binocular rivalry stimulus (Figure 1), in which a face was presented to one eye and a house to the other eye. They also viewed a control stimulus that physically changed from face to house and vice versa. Considering that faces and houses are processed in anatomically separate regions in the occipital and temporal lobe (fMRI [9, 35, 36]; intracranial recordings in humans [37–40]; review [41, 42]) and that perception is reflected in high-frequency power (intracranial recordings in humans [43, 44]; in monkeys [16, 45]), we anticipated to find electrodes that exhibit an increase in high-frequency power (50–130 Hz) for one of the percepts only (either face or house). We performed detailed analysis of the shape and timing of such modulations and found that responses to illusory changes indeed exhibited a characteristic slow and gradual rise. Furthermore, the temporal ordering of responses to illusory changes suggested a reversed-hierarchy cascade of activity, in which higher order ventral regions responded before lower order occipital regions.

RESULTS

Perception-Tuned Responses Localize to the Same Electrodes for Physical and Illusory Changes

In both participants, we found high-frequency (50–130 Hz) power changes associated with perceptual changes on a subset of occipital and posterior temporal electrodes (amounting to 13 and 14 electrodes in participant A and B, respectively; Figures 2A and 2B; see Figures S2B and S2C for analysis of low-frequency power changes). These electrodes were either localized laterally, covering lateral extrastriate visual cortex (electrode names starting with a or b), or ventrally, potentially covering the fusiform face area [42] or the parahippocampal place area [36] (electrode names starting with c or d; anatomical landmarks were used to determine which part of the cortex was covered; see STAR Methods).

Among these electrodes, we found two main response patterns. There were electrodes that responded to physical, but

Please cite this article in press as: de Jong et al., Intracranial Recordings Reveal Unique Shape and Timing of Responses in Human Visual Cortex during Illusory Visual Events, Current Biology (2020), https://doi.org/10.1016/j.cub.2020.05.082

CellPress

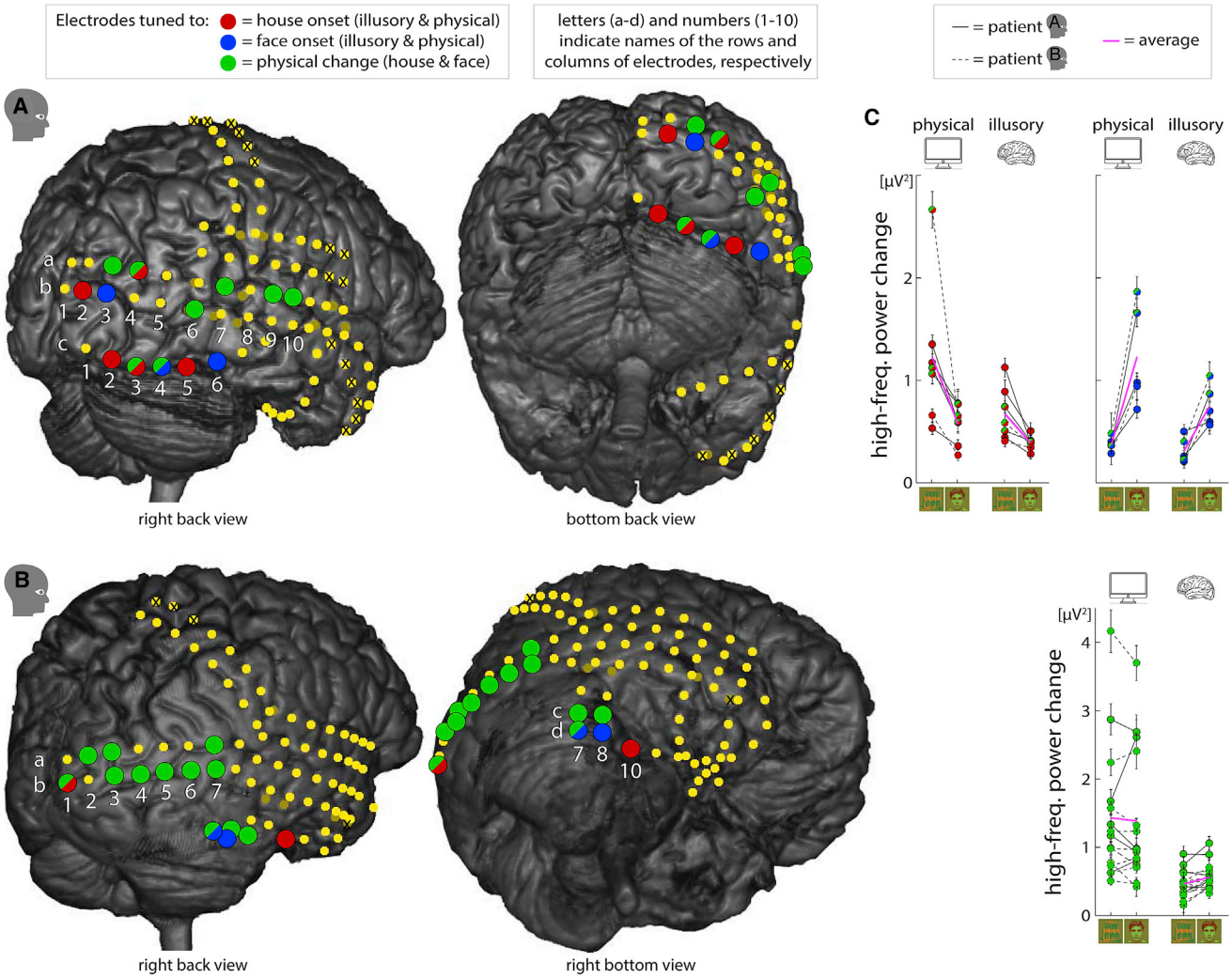

Figure 2. Perception-Tuned Responses Localize to the Same Electrodes for Physical and Illusory Changes

(A and B) Locations of electrodes with broadband high-frequency power changes (50–130 Hz) tuned to certain perceptual changes (participant A in A; participant B in B). Rows and columns of electrode locations are indicated by white letters (a–d) and numbers (1–10), respectively (a and b indicate lateral visual cortex; c and d indicate ventral visual cortex, potentially including fusiform face area and parahippocampal place area). Red and blue circles, electrodes with perception-tuned responses, i.e., responses tuned to onset of either the house (red) or the face (blue) percept, regardless of whether the change was physical or illusory. Green circles, electrodes with responses to physical changes only, regardless of whether the face or the house image appeared. Half-green, half-red/blue circles, electrodes with a combination of both tuning patterns, i.e., perception-tuned responses were higher in amplitude for physical than for illusory changes. For illustration purposes, some ventral electrodes are drawn on top of the cerebellum, although they were in between cerebellum and cortex. Dark yellow circles, electrodes excluded from analysis because they were on top of another electrode grid and did not cover cortex. Bright yellow circles with X mark, electrodes excluded for other reasons (see STAR Methods for criteria). Bright yellow circles without X mark, electrodes without responses tuned to certain perceptual changes (see legend of Figure S2A for analysis of these electrodes). Small head icons indicate participant code. Epochs aligned to the report are presented in Figure S1.

(C) High-frequency power changes for individual electrodes tuned to house onsets (top left), face onsets (top right), and physical changes (bottom). From left to right, each graph shows peak amplitudes for physical house onsets, physical face onsets, illusory house onsets, and illusory face onsets. Solid and dashed lines indicate electrodes in participant A and B, respectively. Note that we present peak amplitudes, meaning that small positive values likely reflect fluctuations in background activity rather than event-related changes. Error bars indicate ±SEM (across epochs). Figure S2 provides more information on tuning of individual electrodes.

not illusory, changes, regardless of whether the stimulus changed from face to house or vice versa (Figures 2A and 2B, green electrodes; Figure 2C, bottom). We did not find any electrodes that responded to illusory, but not physical, changes. In addition, there were electrodes with responses tuned to perception: they either responded to house onsets only or face onsets only, regardless of whether the change was physical or illusory (Figures 2A and 2B, red and blue electrodes, respectively; Figure 2C, top). Some electrodes showed a combination of both tuning patterns (half-green, half-red/blue electrodes in Figure 2; Figure S2A provides more information on tuning of individual electrodes). There was one electrode that responded to all

Please cite this article in press as: de Jong et al., Intracranial Recordings Reveal Unique Shape and Timing of Responses in Human Visual Cortex during Illusory Visual Events, Current Biology (2020), https://doi.org/10.1016/j.cub.2020.05.082

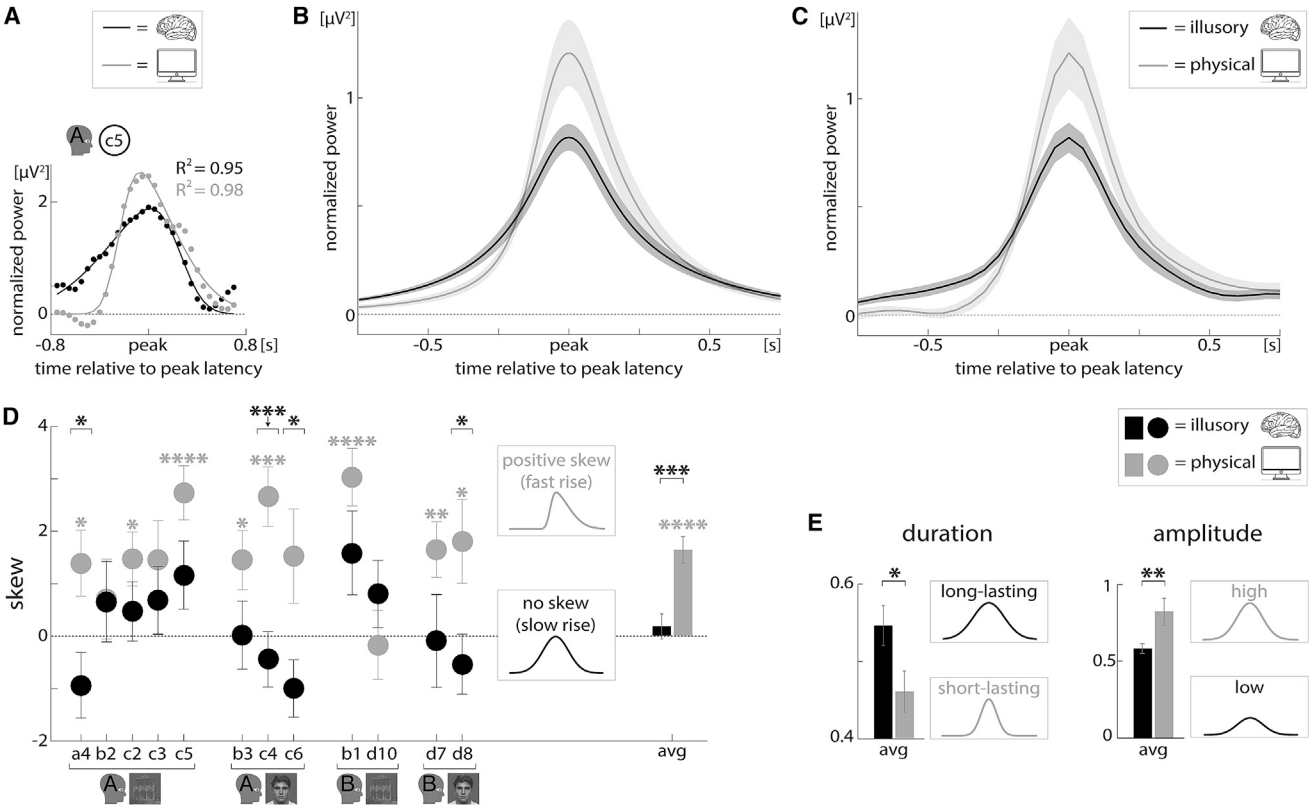

Figure 3. Perception-Tuned Responses to Illusory Changes Rise Characteristically Slowly

(A) Example of single-epoch data (dots) and fitted skewed Gaussians (lines) for an illusory (black) and a physical (gray) change to the preferred percept (data from electrode c5 in participant A).

(B) The averaged shape of skewed Gaussian distributions that best fitted single-epoch responses to illusory (black) and physical (gray) onsets of the preferred percept (average across epochs and across all 12 electrodes with perception-tuned responses found in both participants; Figures 2A and 2B). Responses to illusory changes rise slowly in comparison with the steep high-amplitude rise of responses to physical changes. Time is represented relative to the peak in the single-epoch fits and not relative to the report, to bypass influences of reaction times (indicated by "peak" on the horizontal axis; Figure S3B shows analysis relative to report). Shading indicates ±SEM (across electrodes). Individual electrodes are in (D) and Figure S3A.

(C) The average of the actual responses recorded when illusory (black) and physical (gray) onsets of the preferred percept occurred (averaged across epochs and electrodes with perception-tuned responses in both participants). Conventions are as in (B). Figure S1 presents epochs aligned to the report.

(D) For each individual electrode with perception-tuned responses, we here present the skew of the fitted skewed Gaussians for illusory (black) and physical (gray) onsets of the preferred percept. Responses to physical changes had a positive skew (fast rise and slow decay), whereas responses to illusory changes were symmetrical, i.e., had no skew (slow rise and slow decay). Cartoon curves qualitatively illustrate differences in shape. *$p < 0.05$; **$p < 0.01$; ***$p < 0.001$; ****$p < 0.0001$. Asterisks on top of brackets represent difference between physical and illusory changes. Asterisks just above bar/dot represent difference from zero for that bar/dot. Error bars indicate ±SEM (across epochs for dots; across electrodes for bars).

(E) Duration (i.e., width; left) and amplitude (right) of fitted skewed Gaussians for illusory (black) and physical (gray) onsets of the preferred percept (averaged across epochs and electrodes with perception-tuned responses in both participants). Responses to illusory changes were longer lasting and lower in amplitude. Asterisks represent difference between physical and illusory changes. All individual bars differ from zero (statistics not shown). Conventions are as in (D). Individual electrodes are in Figure S3A.

perceptual changes (see legend of Figure S2A; these responses likely reflected the manual report of the participant as the electrode covered the postcentral sulcus in participant B).

Perception-Tuned Responses to Illusory Changes Rise Characteristically Slowly

There is a large discrepancy between illusory and physical changes regarding how precisely we know when they occurred. Naturally, whereas the timing of physical changes is under our explicit experimental control, illusory changes are initiated in the brain of the observer. Therefore, we know precisely that physical changes are initiated when we change the stimulus on the screen, but our knowledge of the timing of illusory changes is restricted to the observer's report. Unfortunately, the delay between neural activations and the observer's report is largely determined by reaction time. This creates a long-standing problem in the study of binocular rivalry, because reaction times are thought to be relatively slow and variable for illusory compared to physical changes [27–29]. In addition, reaction times may differ between house and face reports (Figure S1A, bottom). The shape of responses averaged across epochs aligned to the report will reflect the magnitude and variability of reaction times in addition to neural effects (specifically, for illusory changes, averaged epochs will be longer lasting and earlier relative to

Please cite this article in press as: de Jong et al., Intracranial Recordings Reveal Unique Shape and Timing of Responses in Human Visual Cortex during Illusory Visual Events, Current Biology (2020), https://doi.org/10.1016/j.cub.2020.05.082

CellPress

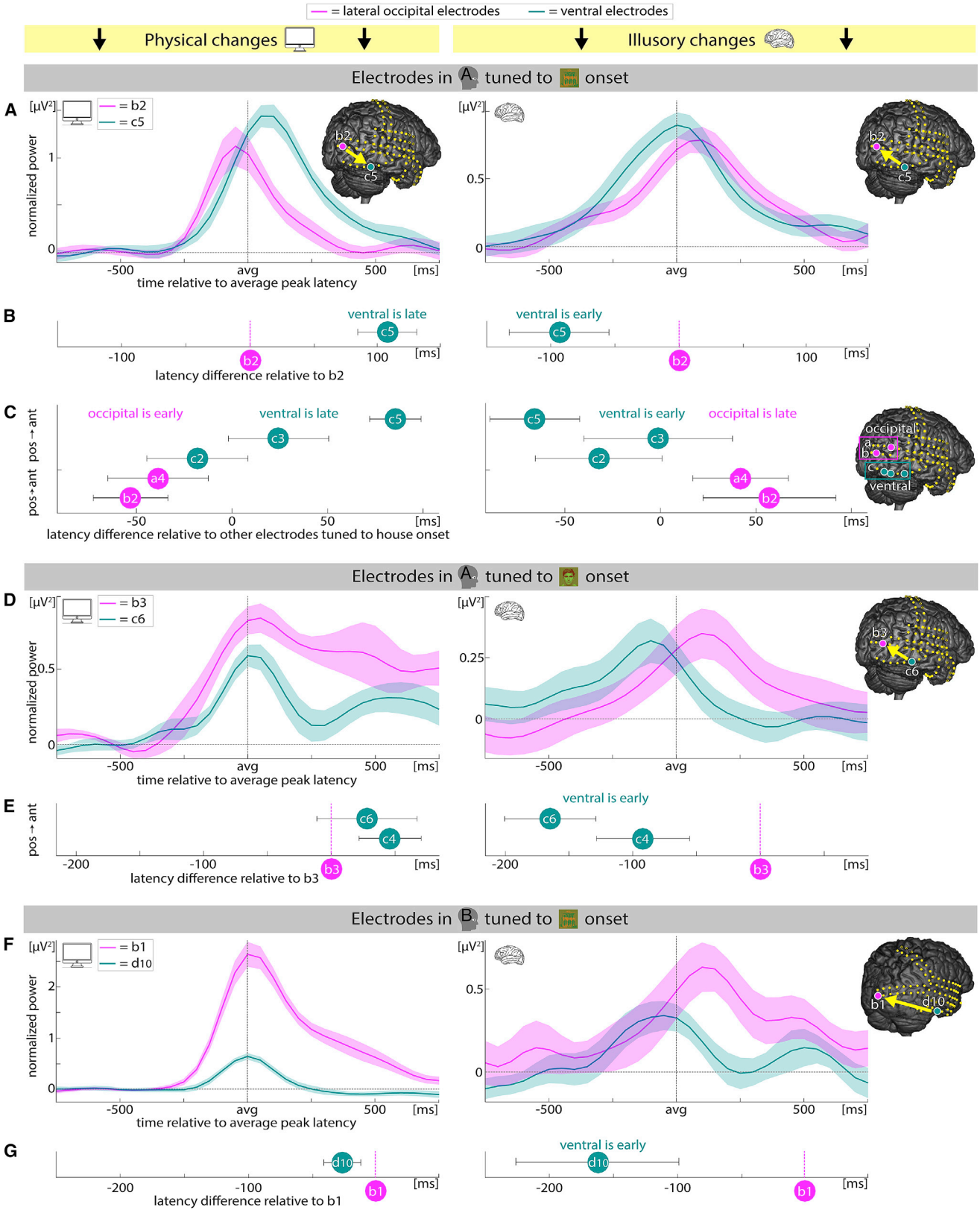

(legend on next page)

Please cite this article in press as: de Jong et al., Intracranial Recordings Reveal Unique Shape and Timing of Responses in Human Visual Cortex during Illusory Visual Events, Current Biology (2020), https://doi.org/10.1016/j.cub.2020.05.082

the report; Figures S1 and S3B). Therefore, it is crucial to analyze the shape of single-epoch responses, irrespective of the latency of the epoch relative to the report. Fortunately, the high signal-to-noise ratio of intracranial recordings enabled us to perform such analyses.

We quantified the shape of the responses to illusory and physical changes by fitting skewed Gaussians to single epochs and analyzing the amplitude, duration (width), and skew of the fitted responses (see STAR Methods; used time window was centered on the single-epoch response peak; median variance explained was 0.75, across electrodes and epochs). Whereas responses to physical changes were skewed to the right, exhibiting a fast rise and a slow decay, responses to illusory changes were symmetrical (unskewed), rising equally slowly as they decay (illusory versus physical: $t_{(11)} = -4.4$, $p = 0.001$; physical: $t_{(11)} = 6.5$, $p = 0.00005$; illusory: $t_{(11)} = 0.8$, $p = 0.4$; tests across electrodes with perception-tuned responses). Responses to illusory changes were also longer lasting ($t_{(11)} = 2.5$; $p = 0.03$) and lower in amplitude ($t_{(11)} = -3.2$; $p = 0.008$) than responses to physical changes (Figure 3). The magnitude of these differences in response shape between physical and illusory changes differed between individual electrodes, but it did not systematically differ between participants (all $t_{(10)} < 1.3$; all $p > 0.2$) or between lateral occipital and ventral electrodes (all $t_{(10)} \leq 1.8$; all $p > 0.1$; Figures 3D and S3A). The slow rise of responses to illusory changes was thus found across the visual hierarchy. Next, we analyzed differences in response timing between perception-tuned electrodes.

Perception-Tuned Responses to Illusory Changes Occur in a Reversed-Hierarchy Order

We analyzed response latencies for single electrodes on single epochs (i.e., for each report of a perceptual change individually). We were not interested in the absolute latencies of the neural response (delay to report), as these are largely determined by reaction time (see Figure S1). Crucially, we compared responses on different electrodes that were tuned to the same percept in the same participant and asked the question: did electrodes activate sequentially to each report and, if so, in which order did they activate? For each possible pair of electrodes, we analyzed the temporal order in which they responded to physical and illusory changes, thereby allowing a direct comparison, irrespective of possible differences in reaction times. The present dataset is suited for such analysis, in contrast to conventional recording techniques that lack either the needed spatial coverage (monkey electrophysiology) or the spatial/temporal resolution and signal-to-noise ratio (fMRI and scalp recordings).

We observed a striking difference between physical and illusory changes for pairs of electrodes that consisted of one lateral occipital electrode and one ventral electrode. Illusory changes were associated with a "reversed-hierarchy" latency difference in which ventral electrodes (which covered posterior fusiform or parahippocampal regions) peaked earlier than lateral occipital electrodes (Figure 4; right column). In contrast, for physical changes, lateral occipital responses either preceded ventral responses or occurred at a similar latency, in accordance with a fast "bottom-up" processing stream (Figure 4; left column; bottom-up processing is further supported by the presence of early perception-invariant responses; see Figure 5). Below, we will discuss these results per participant, per percept. We first show results for house onsets in participant A (2 lateral occipital electrodes, 3 ventral electrodes; Figures 4A–4C), then for face onsets in participant A (1 lateral occipital electrode, 2 ventral electrodes; Figures 4D and 4E), and then for house onsets in participant B (1 lateral occipital electrode, 1 ventral electrode; Figures 4F and 4G). Regarding face onsets in participant B, we could not compare ventral with lateral occipital response

Figure 4. Perception-Tuned Responses to Illusory Changes Occur in a Reversed-Hierarchy Order

(A) High-frequency power changes of two electrodes with responses tuned to house onsets in participant A: lateral occipital electrode b2, estimated to cover secondary visual cortex (pink lines), and ventral electrode c5, estimated to cover posterior fusiform gyrus (cyan lines; see STAR Methods for localization procedures). Per report, responses are aligned in time to the averaged peak latency of b2 and c5 (indicated by "avg" on the horizontal axis). Figure S1C (top) presents responses aligned to the report. Shading indicates ± SEM (across epochs). (A)–(G) show physical changes on the left, illusory changes on the right, lateral occipital electrodes in pink, and ventral electrodes in green.

(B) Single-epoch peak latency differences derived from responses shown in (A). Compared with lateral occipital electrode b2 (pink dot), ventral electrode c5 (cyan dot) peaked about 100 ms later in response to physical house onsets (left graph) and about 100 ms earlier in response to illusory house onsets (right graph). This suggests a reversed-hierarchy processing stream for illusory house onsets. Error bars indicate ±SEM (across epochs).

(C) Averaged peak latency differences for all 5 electrodes with responses tuned to house onsets in participant A. The order in which these electrodes peaked was reversed for illusory compared to physical house onsets, suggesting activation cascades that travel in opposite directions. For each electrode, the average difference in single-epoch peak latency relative to the other 4 electrodes is presented (e.g., in response to illusory house onsets b2 on average peaked >50 ms later than the other 4 electrodes). Along the vertical axis, electrodes are ordered according to their location: lateral occipital (pink circles) to ventral (cyan circles) and posterior ("pos") to anterior ("ant"). Error bars indicate ±SEM (across pairs of electrodes).

(D) High-frequency power changes of two electrodes in participant A with responses tuned to face onsets: lateral occipital electrode b3, estimated to cover secondary visual cortex, and ventral electrode c6, estimated to cover posterior fusiform gyrus. Conventions are as in (A).

(E) Single-epoch peak latency differences between lateral occipital electrode b3 and ventral electrodes c4 and c6, which all had responses tuned to face onsets in participant A. Both ventral electrodes peaked earlier than the lateral occipital electrode in response to illusory changes (in line with A–C). Peak latencies for physical face onsets were similar. Conventions are as in (B).

(F) High-frequency power changes of two electrodes in participant B with responses tuned to house onsets: lateral occipital electrode b1, estimated to cover secondary visual cortex, and ventrotemporal electrode d10, estimated to cover fusiform/parahippocampal gyrus. Note the high amplitude of the response of b1 to physical house onsets, reflecting that perception preference on this electrode was stronger for physical than for illusory changes (Figures S2A and 2B). Conventions are as in (A). Figure S1C (bottom) presents responses aligned to the report.

(G) Single-epoch peak latency differences between lateral occipital electrode b1 and ventral electrode d10 in response to physical and illusory house onsets in participant B. For illusory house onsets, the ventral electrode peaked earlier than the lateral occipital electrode, although peak latencies for physical house onsets were similar. Conventions are as in (B). Face onsets in participant B are not shown, because this participant had no lateral occipital electrode with responses tuned to face onsets (see Figure 2B).

Please cite this article in press as: de Jong et al., Intracranial Recordings Reveal Unique Shape and Timing of Responses in Human Visual Cortex during Illusory Visual Events, Current Biology (2020), https://doi.org/10.1016/j.cub.2020.05.082

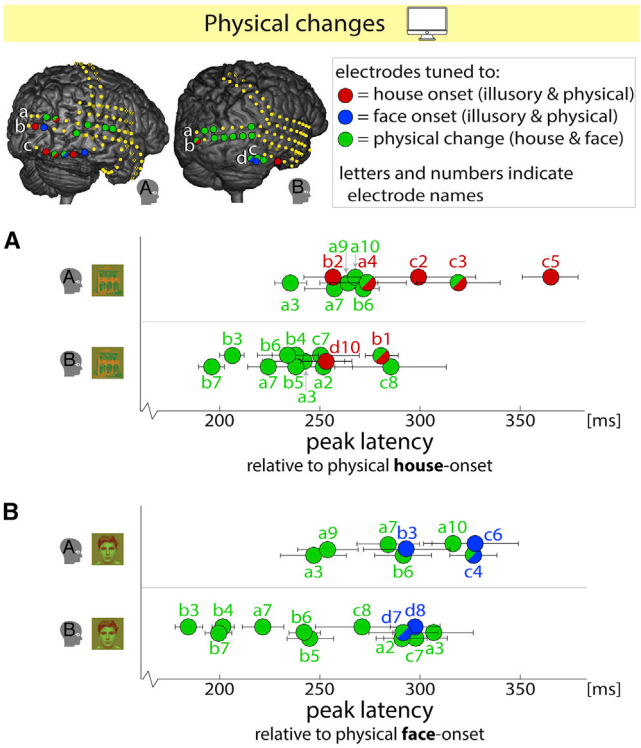

Figure 5. Physical Changes Are Associated with Early Responses that Are Invariant to Perception

(A and B) Peak latencies in response to physical house (A) and face (B) onsets. For both image onsets and both participants, electrodes with responses tuned to physical changes (green dots) peaked earlier than electrodes with perception-tuned responses (red/blue dots; head icons indicate participant code). Color coding of electrodes is as in Figure 2. Error bars indicate ±SEM (across epochs). See Figure 4 for peak latencies associated with illusory changes.

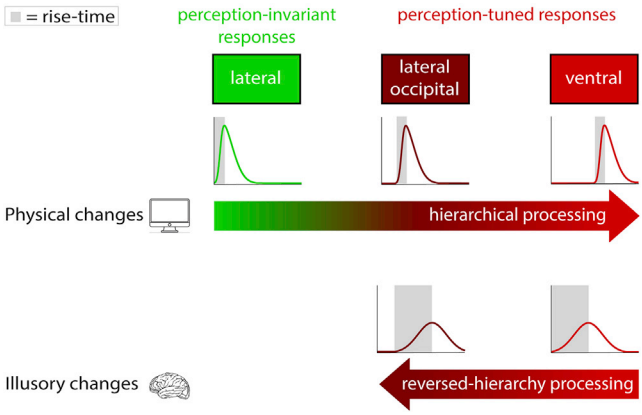

Figure 6. Summary of Main Findings

Top row: physical changes elicited high-amplitude responses with a relatively fast rise (Figure 3; gray shading indicates rise time), arguably reflecting their abrupt and unequivocal onset. The responses were temporally (Figures 4 and 5) and spatially (Figure 2) ordered along a hierarchical processing stream: early lateral responses were perception invariant (green), and later lateral (dark red) and ventral (bright red) responses were perception tuned. Perception-tuned responses in lateral occipital regions on some occasions preceded those in ventral regions (Figures 4A–4C). Bottom row: illusory changes elicited perception-tuned responses only. These occurred on the same electrodes and with the same percept preference as physical changes (Figure 2), suggesting the same regions were involved. However, in comparison to physical changes, the rise of responses was characteristically slow (Figure 3). We tentatively link this to network-wide gradual destabilization of the dominant percept (and a concomitant slow rise of activity tuned to the upcoming percept). Furthermore, perception-tuned responses in ventral regions consistently preceded those in lateral occipital regions (Figure 4), suggesting a reversed-hierarchy processing stream. We speculate this reflects a subsequent stabilization stage, in which feedback signals graduate the new percept. Findings are qualitatively illustrated by the arrows and cartoon curves.

latencies, as there were no lateral occipital electrodes with responses tuned to face onsets in this participant (Figure 2B).

In participant A, responses on ventral electrodes c2, c3, and c5 (all estimated to cover posterior fusiform gyrus) and lateral occipital electrodes b2 and a4 (estimated to cover secondary visual cortex [V2] and visual area 3 [V3], respectively) were all tuned to house onsets (Figure 2A; see STAR Methods for localization procedures). The above-mentioned difference in temporal ordering between physical and illusory changes was most robust for electrode c5, which is the most anterior ventral electrode (repeated-measures ANOVA over epochs; within factor electrode × between factor type of change; c5 compared with both lateral occipital electrodes: both $F \geq 13.5$, both $p = 0.0006$; c3-a4 and c2-b2: both $F \geq 4.7$, both $p < 0.04$; c2-a4 and c3-b2: both $F \leq 1.9$, both $p \geq 0.2$). To appreciate the magnitude of the observed latency differences, consider that responses to physical house onsets peaked 106 ± 23 ms SEM *later* ($t_{(15)} = 4.6$; $p = 0.0004$) on ventral electrode c5 than on lateral occipital electrode b2. In contrast, responses to illusory house onsets peaked 95 ± 39 ms SEM *earlier* ($t_{(27)} = -2.4$; $p = 0.02$) on c5 than on b2, yielding a total difference between illusory and physical house onsets of 201 ms (Figures 4A and 4B). Per-electrode averaging of latency differences relative to each of the other 4 electrodes corroborated a bottom-up (lateral to ventral) processing stream for physical changes (temporal order of electrodes: b2-a4-c2-c3-c5) and the reversed, top-down stream for illusory changes (temporal order of electrodes: c5-c2-c3-a4-b2; Figure 4C).

Regarding illusory face onsets in participant A, responses on ventral electrodes c4 and c6 (both estimated to cover posterior fusiform cortex) peaked earlier than responses on lateral occipital electrode b3 (estimated to cover secondary visual cortex; Figures 4D and 4E). Specifically, electrodes c6 peaked 165 ± 36 ms SEM earlier ($t_{(26)} = -4.6$; $p = 0.00009$) and electrode c4 peaked 92 ± 36 ms SEM earlier ($t_{(31)} = -2.5$; $p = 0.02$) than electrode b3 (electrode × type of change: c6-b3, $F_{(1,34)} = 8.5$, $p = 0.006$; c4-b3, $F_{(1,43)} = 5.4$, $p = 0.03$). Peak latencies for physical face onsets were similar (c6-b3 and c4-b3: both $t > 1.9$, both $p > 0.08$).

In participant B, responses to illusory house onsets on ventral electrode d10 (estimated to cover fusiform/parahippocampal gyrus) peaked 162 ± 64 ms SEM earlier ($t_{(11)} = -2.5$; $p = 0.03$) than responses on lateral occipital electrode b1 (estimated to cover secondary visual cortex; Figures 4F and 4G; electrode × type of change: $F_{(1,28)} = 6.3$; $p = 0.02$). Peak latencies for physical house onsets were similar (d10-b1: $t_{(17)} = -1.7$; $p = 0.11$).

For within-region pairs of electrodes, i.e., pairs consisting of two lateral occipital electrodes or two ventral electrodes, we found no differences in temporal ordering between illusory and

Please cite this article in press as: de Jong et al., Intracranial Recordings Reveal Unique Shape and Timing of Responses in Human Visual Cortex during Illusory Visual Events, Current Biology (2020), https://doi.org/10.1016/j.cub.2020.05.082

physical changes (electrode × type of change: all $F \leq 1.2$, all $p \geq 0.3$), with the following two exceptions. In participant A, electrode c5 peaked earlier than c3 for illusory house onsets ($t_{(33)} = -2.9$; $p = 0.007$), although peak latencies for physical house onsets were similar ($t_{(12)} = 1.6$; $p = 0.1$; electrode × type of change: $F_{(1,45)} = 6.8$, $p = 0.01$). In participant B, electrode d8 peaked later than d7 for illusory face onsets ($t_{(24)} = 3.9$; $p = 0.0007$), although peak latencies for physical face onsets were similar ($t_{(18)} = -0.4$; $p = 0.7$; electrode × type of change: $F_{(1,42)} = 10.9$, $p = 0.002$).

Physical Changes Are Associated with Early Responses that Are Invariant to Perception

As mentioned above, some electrodes responded only to physical changes and not to illusory changes. In both participants and for physical house as well as physical face onsets, these stimulus-based responses peaked *earlier* than perception-tuned responses (Figure 5; latencies relative to the moment of the on-screen change). Specifically, for physical house onsets, the average latency difference was 24 ms in participant A (test across epochs and electrodes: $t_{(373)} = 3.2$, $p = 0.00$; ANOVA over electrodes: $F_{(9,186)} = 5.6$, $p \approx 0$) and 31 ms in participant B ($t_{(447)} = 3.2$, $p = 0.001$; $F_{(7,141)} = 2.5$, $p = 0.02$). For physical face onsets, the average latency difference was 37 ms in participant A ($t_{(305)} = 1.2$, $p = 0.2$; $F_{(11,223)} = 2.8$, $p = 0.002$) and 48 ms in participant B ($t_{(440)} = 4.1$, $p = 0.00004$; $F_{(11,212)} = 10.3$, $p \approx 0$).

DISCUSSION

Binocular rivalry is hallmarked by the perception of illusory changes in the stimulus. Comparing these illusory changes with physical stimulus changes, we found that both elicited perception-tuned, high-frequency (50–130 Hz) responses at the same posterior electrode sites. The temporal characteristics of these responses, however, showed marked differences (summarized in Figure 6). In the following paragraphs, we tentatively suggest these differences reflect two processing stages of illusory changes: gradual *destabilization* of the current percept, followed by top-down *stabilization* of the new percept.

Physical Changes Are Associated with a Bottom-Up, Hierarchical, Processing Stream

Physical changes elicited two distinct response patterns that together point to a hierarchical processing stream: early perception-invariant responses and later perception-tuned responses (Figures 2 and 5). Perception-invariant responses occurred irrespective of whether the face or house image was presented and might reflect early processing of changes in visual input. Illusory changes lack a concomitant change in visual input and did not elicit perception-invariant responses. Perception-tuned responses were found on a largely separate subset of electrodes that covered a network of visual regions along the ventral processing stream (Figure 2; in line with [9, 34, 36, 38–42]). Here, onset of either the face or the house percept elicited a response, irrespective of whether this reflected a physical or illusory change. Lower order occipital regions on some occasions responded earlier than higher order ventral regions [36, 42] (Figures 4A–4C). Responses to physical changes had a relatively fast rise (Figure 3), arguably reflecting the abrupt and unequivocal onset of changes in perception that are triggered by presenting a new stimulus.

Illusory Changes Elicit Responses that Rise Slowly

Illusory changes elicited perception-tuned responses only. These occurred on the same electrodes and with the same percept preference as physical changes (Figure 2), corroborating that the same perception-dedicated neural networks were involved (see Introduction). Alternative response patterns found in monkeys [5, 12, 45] may be averaged out at the spatial meso-scale of the present recordings. Although previous investigations relied on averaged epochs that are influenced by reaction times [13, 46] (which may result in exaggerated differences; Figures S1B, S1C, and S3B), we here eliminated any influence of reaction times by analyzing single-epoch responses, irrespective of their delay to the report.

Across the visual hierarchy, responses to illusory changes were transient but relatively long lasting and low in amplitude. This might reflect increased variability in single-neuron response latencies (in line with responses to illusory and physical changes having a similar area under the curve at the electrode level) [34]. In addition, it could be that illusory changes recruited a smaller subset of neurons covered by an electrode, for example, because perception-invariant neurons were not activated. Conceptually, illusory changes may share some—but not all—characteristics with low-contrast physical changes [29]. However, apart from downscaling and delaying the response, reducing stimulus contrast does not alter the shape of responses to physical stimuli [47–49]. The comparison with low-contrast physical stimuli therefore does not extend to our findings described below (slow rise time and reversed-hierarchy processing stream).

Furthermore, responses to illusory changes exhibited a characteristic slow rise: responses were symmetrical (slow rise and slow decay), whereas responses to physical changes were asymmetrical (fast rise and slow decay; Figure 3). We speculate the slow rise reflects the gradual rather than abrupt nature of illusory changes, both phenomenally and in terms of underlying neural mechanisms. Phenomenally, illusory changes are sometimes reported to appear gradual, with intermediate or mixed percepts being experienced during the perceptual transition [27, 29, 50, 51]. Regarding neural mechanisms, several theoretical accounts of binocular rivalry are compatible with a gradual, network-wide rise of responses tuned to the impending—but still suppressed—percept [25]. First, illusory changes are thought to require reverberating interactions between different levels of the processing hierarchy, rather than being initiated in one specific region [21–24]. Second, predictive coding accounts [25, 52] suggest residual evidence for the suppressed percept leads to ongoing accumulation of prediction errors [26, 53]. Third, following the idea that binocular rivalry involves mutual inhibition between neurons coding for one or the other percept [21, 54], gradual adaptation of neurons coding for the dominant percept may result in progressive disinhibition of neurons coding for the suppressed percept. Fourth, preconscious activity favoring the impending percept may gradually accumulate in a fashion similar to neural activations associated with perceptual decision making [55, 56]. In all, we suggest that the slow rise of responses to illusory changes reflects a destabilization stage in which

Please cite this article in press as: de Jong et al., Intracranial Recordings Reveal Unique Shape and Timing of Responses in Human Visual Cortex during Illusory Visual Events, Current Biology (2020), https://doi.org/10.1016/j.cub.2020.05.082

activity associated with the impending change gradually accumulates across the visual hierarchy.

Illusory Changes Are Associated with a Reversed-Hierarchy (Top-Down) Processing Stream

We compared the temporal order of responses on electrodes tuned to the same percept in the same participant, thereby allowing direct comparison of illusory and physical changes, irrespective of possible differences in reaction times (Figure S1). In contrast to physical changes, perception-tuned responses to illusory changes consistently peaked first in ventral regions and later in lateral occipital regions (Figure 4). This points to a reversed-hierarchy processing cascade, as these ventral regions (posterior fusiform and parahippocampal gyrus) are engaged in final, position- and size-invariant stages of house/face processing, although lateral occipital responses reflect earlier processing stages [36, 41, 42]. Relative timing differences between illusory and physical changes were quite large (~200 ms; Figures 4A and 4B) and seemed unrelated to differences in response shape reported above, which were present in both ventral and lateral occipital regions (Figures 3D and S3A). We do not exclude the possibility of top-down processing in association with physical changes, but when compared with illusory changes, our results indicate a reversed-hierarchy, top-down cascade specifically for the latter.

There has been an intense debate in the literature regarding the role of top-down processing in illusory changes [5, 17, 22, 25, 29, 53]. Some authors argue that initiation of illusory changes requires a governing feedback signal, originating from higher order visual regions [34, 57–59] or anterior non-sensory regions [13, 26, 53, 60, 61]. The relatively long timescale over which the reversed-hierarchy cascade developed (~100 ms; Figure 4) does not point to a governing signal that reaches different visual regions simultaneously. We speculate that the reversed-hierarchy cascade reflects an ultimate rather than an initial stage of processing an illusory change, i.e., a graduation of the destabilization stage proposed above. We tentatively characterize it as a stabilization stage in which signals travel through the visual system in reversed-hierarchy direction to re-coordinate the network in favor of responses tuned to the new percept. This traveling signal may originate in anterior non-sensory regions and travel through fusiform/parahippocampal cortex, eventually reaching occipital cortex, or may originate in fusiform/parahippocampal cortex and travel down the visual hierarchy from there.

Low-Frequency Power Changes Were Invariant to Perception

Decreases in alpha power have previously been linked to feedback processing in monkey visual cortex [62] and perception-tuned responses in certain paradigms [4, 61, 63]. We did not find perception-tuned changes in low-frequency power (legend of Figure S2B), in line with several previous reports [16, 43, 45]. High-frequency modulations often reflect faster and more local processes than low-frequency modulations [64–68], and accordingly, they peaked earlier and were less correlated between neighboring electrodes covering occipital cortex [34]. Electrophysiology in monkeys indicated that perceptual suppression of stimuli is first reflected in high-frequency modulations before it influences low-frequency modulations [61, 63]. The local nature and early timing of high-frequency power changes fits well with a proposed role in fast perceptual dynamics.

Possible Contribution of Other Processes Associated with Perception

It is unlikely that neural processes related to mere motor execution influenced our comparisons, as we juxtapose reports to physical and illusory changes. Furthermore, perception-tuned responses were found in regions dedicated to perception rather than motor processing. However, perceptual processing might be influenced by the task to report each perceptual change. A "no report" paradigm could be useful to investigate this possibility [27, 69]. Attentional modulations or other processes associated with perception, but not directly reflecting perceptual content, may also have contributed [70]. However, perception-tuned responses were found in high-frequency power changes (Figure S2B), although attentional modulations are often associated with low-frequency power changes [71, 72] (but see [73]).

Although participants reported that each eye saw none of the other eyes' image, it is hard to guarantee absence of cross-talk between the eyes. Yet, it is unlikely that cross-talk would elicit perception-tuned, reversed-hierarchy processing. Also, we cannot rule out an influence of eye movements, although previous experiments with similar setup and fixation instructions showed illusory changes occur independently of eye movements [14, 74]. Last, it is unknown whether and how the participants' epileptic condition affected the recordings. Importantly, the analyzed posterior sites did not overlap with epileptic foci in either participant.

Possible Extensions of the Present Study

Face-house binocular rivalry may involve stronger suppression and more feedback processing than rivalry between images of gratings [75]. It would be interesting to investigate whether our results extend to grating rivalry, although the spatial meso-scale of surface recordings is probably insufficient for picking up responses tuned to different grating orientations. Another interesting paradigm to investigate is flash suppression, which involves a stimulus change coinciding with the perceptual change during binocular rivalry. Previous studies in monkeys investigated flash suppression but lacked spatial coverage to assess whether induced perceptual changes involved reversed-hierarchy processing [4, 16, 45, 63]. Another useful extension of our study is functional localization experiments, such as retinotopic mapping, which would enable precise determination of the sampled functional regions.

Summary and Conclusion

Although limited two participants, the present dataset includes simultaneous recording from human occipital and posterior temporal lobe during binocular rivalry. Our results indicate that illusory and physical changes in visual input involve the same perception-dedicated brain regions but in a markedly different manner. In comparison to physical changes, responses to illusory changes had a characteristic slow rise. Furthermore, the processing hierarchy of illusory changes was reversed compared to physical changes, as higher order ventral regions responded earlier than lower order lateral occipital regions. We

tentatively suggest our findings reflect two processing stages associated with processing illusory changes. The first stage could be network-wide gradual destabilization of the dominant percept and concomitant gradual accumulation of neural activity tuned to the alternative percept. The second could be a stabilization stage, in which a directional, reversed-hierarchy cascade of activity graduates the new percept. The proposed two-stage process may unify currently separate theories about the role of feedback processing and communication within and beyond visual cortex during binocular rivalry.

STAR★METHODS

Detailed methods are provided in the online version of this paper and include the following:

- KEY RESOURCES TABLE
- RESOURCE AVAILABILITY
  - Lead contact
  - Materials availability
  - Data and code availability
- EXPERIMENTAL MODEL AND SUBJECT DETAILS
  - Participants
- METHOD DETAILS
  - Illusory changes of the binocular rivalry stimulus
  - Physical changes of the stimulus
  - Procedure
  - Electrocorticographic recording and processing
- QUANTIFICATION AND STATISTICAL ANALYSIS
  - Behavioral analysis
  - Identification and tuning of electrodes
  - Location of electrodes
  - The shape of responses
  - The timing of responses

SUPPLEMENTAL INFORMATION

Supplemental Information can be found online at https://doi.org/10.1016/j.cub.2020.05.082.

ACKNOWLEDGMENTS

This work was supported by Dutch Research Council (NWO) CAS grant 012.200.012 awarded to T.K., Amsterdam Brain and Mind Project (ABMP) grant 2015-7 awarded to T.K., Royal Netherlands Academy of Arts and Sciences (KNAW) Ammodo Award awarded to S.O.D., and Dutch Research Council (NWO) VICI grant 016.Vici.185.050 awarded to S.O.D.

AUTHOR CONTRIBUTIONS

Conceptualization, M.C.d.J., T.K., and S.O.D.; Methodology, Software, and Formal Analysis, M.C.d.J.; Investigation, M.J.V. and F.S.S.L.; Resources, F.S.S.L., N.F.R., and R.v.E.; Writing – Original Draft, M.C.d.J.; Writing – Review & Editing, all authors; Funding Acquisition, T.K. and S.O.D.

DECLARATION OF INTERESTS

The authors declare no competing interests.

Received: December 4, 2019
Revised: May 1, 2020
Accepted: May 27, 2020
Published: July 2, 2020

REFERENCES

1. Hering, E. (1864). Vom binocularen Tiefsehen. Kritik einer Abhandlung von Helmholtz über den Horopter (Beiträge zur Physiologie V, Wilhelm Engelmann).
2. Haynes, J.D., Deichmann, R., and Rees, G. (2005). Eye-specific effects of binocular rivalry in the human lateral geniculate nucleus. Nature *438*, 496–499.
3. Wunderlich, K., Schneider, K.A., and Kastner, S. (2005). Neural correlates of binocular rivalry in the human lateral geniculate nucleus. Nat. Neurosci. *8*, 1595–1602.
4. Maier, A., Wilke, M., Aura, C., Zhu, C., Ye, F.Q., and Leopold, D.A. (2008). Divergence of fMRI and neural signals in V1 during perceptual suppression in the awake monkey. Nat. Neurosci. *11*, 1193–1200.
5. Leopold, D.A., and Logothetis, N.K. (1996). Activity changes in early visual cortex reflect monkeys' percepts during binocular rivalry. Nature *379*, 549–553.
6. Polonsky, A., Blake, R., Braun, J., and Heeger, D.J. (2000). Neuronal activity in human primary visual cortex correlates with perception during binocular rivalry. Nat. Neurosci. *3*, 1153–1159.
7. Tong, F., and Engel, S.A. (2001). Interocular rivalry revealed in the human cortical blind-spot representation. Nature *411*, 195–199.
8. Haynes, J.D., and Rees, G. (2005). Predicting the stream of consciousness from activity in human visual cortex. Curr. Biol. *15*, 1301–1307.
9. Tong, F., Nakayama, K., Vaughan, J.T., and Kanwisher, N. (1998). Binocular rivalry and visual awareness in human extrastriate cortex. Neuron *21*, 753–759.
10. Kreiman, G., Fried, I., and Koch, C. (2002). Single-neuron correlates of subjective vision in the human medial temporal lobe. Proc. Natl. Acad. Sci. USA *99*, 8378–8383.
11. Sheinberg, D.L., and Logothetis, N.K. (1997). The role of temporal cortical areas in perceptual organization. Proc. Natl. Acad. Sci. USA *94*, 3408–3413.
12. Logothetis, N.K., and Schall, J.D. (1989). Neuronal correlates of subjective visual perception. Science *245*, 761–763.
13. Gelbard-Sagiv, H., Mudrik, L., Hill, M.R., Koch, C., and Fried, I. (2018). Human single neuron activity precedes emergence of conscious perception. Nat. Commun. *9*, 2057.
14. Brouwer, G.J., and van Ee, R. (2007). Visual cortex allows prediction of perceptual states during ambiguous structure-from-motion. J. Neurosci. *27*, 1015–1023.
15. Libedinsky, C., and Livingstone, M. (2011). Role of prefrontal cortex in conscious visual perception. J. Neurosci. *31*, 64–69.
16. Panagiotaropoulos, T.I., Deco, G., Kapoor, V., and Logothetis, N.K. (2012). Neuronal discharges and gamma oscillations explicitly reflect visual consciousness in the lateral prefrontal cortex. Neuron *74*, 924–935.
17. Naber, M., and Brascamp, J. (2015). Commentary: is the frontal lobe involved in conscious perception? Front. Psychol. *6*, 1736.
18. Boly, M., Massimini, M., Tsuchiya, N., Postle, B.R., Koch, C., and Tononi, G. (2017). Are the neural correlates of consciousness in the front or in the back of the cerebral cortex? Clinical and neuroimaging evidence. J. Neurosci. *37*, 9603–9613.
19. Yoshor, D., Bosking, W.H., Ghose, G.M., and Maunsell, J.H. (2007). Receptive fields in human visual cortex mapped with surface electrodes. Cereb. Cortex *17*, 2293–2302.
20. Martinovic, J., and Busch, N.A. (2011). High frequency oscillations as a correlate of visual perception. Int. J. Psychophysiol. *79*, 32–38.
21. Blake, R., and Logothetis, N. (2002). Visual competition. Nat. Rev. Neurosci. *3*, 13–21.
22. Tong, F., Meng, M., and Blake, R. (2006). Neural bases of binocular rivalry. Trends Cogn. Sci. *10*, 502–511.

23. Wang, M., Arteaga, D., and He, B.J. (2013). Brain mechanisms for simple perception and bistable perception. Proc. Natl. Acad. Sci. USA *110*, E3350–E3359.

24. Panagiotaropoulos, T.I., Kapoor, V., and Logothetis, N.K. (2014). Subjective visual perception: from local processing to emergent phenomena of brain activity. Philos. Trans. R. Soc. Lond. B Biol. Sci. *369*, 20130534.

25. Brascamp, J., Sterzer, P., Blake, R., and Knapen, T. (2018). Multistable perception and the role of the frontoparietal cortex in perceptual inference. Annu. Rev. Psychol. *69*, 77–103.

26. Weilnhammer, V., Stuke, H., Hesselmann, G., Sterzer, P., and Schmack, K. (2017). A predictive coding account of bistable perception - a model-based fMRI study. PLoS Comput. Biol. *13*, e1005536.

27. Naber, M., Frässle, S., and Einhäuser, W. (2011). Perceptual rivalry: reflexes reveal the gradual nature of visual awareness. PLoS ONE *6*, e20910.

28. Kornmeier, J., and Bach, M. (2006). Bistable perception – along the processing chain from ambiguous visual input to a stable percept. Int. J. Psychophysiol. *62*, 345–349.

29. Knapen, T., Brascamp, J., Pearson, J., van Ee, R., and Blake, R. (2011). The role of frontal and parietal brain areas in bistable perception. J. Neurosci. *31*, 10293–10301.

30. Lachaux, J.P., Axmacher, N., Mormann, F., Halgren, E., and Crone, N.E. (2012). High-frequency neural activity and human cognition: past, present and possible future of intracranial EEG research. Prog. Neurobiol. *98*, 279–301.

31. Crone, N.E., Korzeniewska, A., and Franaszczuk, P.J. (2011). Cortical γ responses: searching high and low. Int. J. Psychophysiol. *79*, 9–15.

32. Quiroga, R.Q., Mukamel, R., Isham, E.A., Malach, R., and Fried, I. (2008). Human single-neuron responses at the threshold of conscious recognition. Proc. Natl. Acad. Sci. USA *105*, 3599–3604.

33. Reber, T.P., Faber, J., Niediek, J., Boström, J., Elger, C.E., and Mormann, F. (2017). Single-neuron correlates of conscious perception in the human medial temporal lobe. Curr. Biol. *27*, 2991–2998.e2.

34. de Jong, M.C., Hendriks, R.J., Vansteensel, M.J., Raemaekers, M., Verstraten, F.A., Ramsey, N.F., Erkelens, C.J., Leijten, F.S., and van Ee, R. (2016). Intracranial recordings of occipital cortex responses to illusory visual events. J. Neurosci. *36*, 6297–6311.

35. Kanwisher, N., McDermott, J., and Chun, M.M. (1997). The fusiform face area: a module in human extrastriate cortex specialized for face perception. J. Neurosci. *17*, 4302–4311.

36. Epstein, R.A. (2008). Parahippocampal and retrosplenial contributions to human spatial navigation. Trends Cogn. Sci. *12*, 388–396.

37. Pourtois, G., Spinelli, L., Seeck, M., and Vuilleumier, P. (2010). Modulation of face processing by emotional expression and gaze direction during intracranial recordings in right fusiform cortex. J. Cogn. Neurosci. *22*, 2086–2107.

38. Miller, K.J., Hermes, D., Witthoft, N., Rao, R.P., and Ojemann, J.G. (2015). The physiology of perception in human temporal lobe is specialized for contextual novelty. J. Neurophysiol. *114*, 256–263.

39. Miller, K.J., Schalk, G., Hermes, D., Ojemann, J.G., and Rao, R.P. (2016). Spontaneous decoding of the timing and content of human object perception from cortical surface recordings reveals complementary information in the event-related potential and broadband spectral change. PLoS Comput. Biol. *12*, e1004660.

40. Miller, K.J., Hermes, D., Pestilli, F., Wig, G.S., and Ojemann, J.G. (2017). Face percept formation in human ventral temporal cortex. J. Neurophysiol. *118*, 2614–2627.

41. Haxby, J.V., Hoffman, E.A., and Gobbini, M.I. (2000). The distributed human neural system for face perception. Trends Cogn. Sci. *4*, 223–233.

42. Grill-Spector, K., Weiner, K.S., Kay, K., and Gomez, J. (2017). The functional neuroanatomy of human face perception. Annu. Rev. Vis. Sci. *3*, 167–196.

43. Lachaux, J.P., George, N., Tallon-Baudry, C., Martinerie, J., Hugueville, L., Minotti, L., Kahane, P., and Renault, B. (2005). The many faces of the gamma band response to complex visual stimuli. Neuroimage *25*, 491–501.

44. Matsuzaki, N., Juhász, C., and Asano, E. (2012). Oscillatory modulations in human fusiform cortex during motion-induced blindness: intracranial recording. Clin. Neurophysiol. *123*, 1925–1930.

45. Keliris, G.A., Logothetis, N.K., and Tolias, A.S. (2010). The role of the primary visual cortex in perceptual suppression of salient visual stimuli. J. Neurosci. *30*, 12353–12365.

46. Strüber, D., and Herrmann, C.S. (2002). MEG alpha activity decrease reflects destabilization of multistable percepts. Brain Res. Cogn. Brain Res. *14*, 370–382.

47. Zhou, J., Benson, N.C., Kay, K., and Winawer, J. (2019). Predicting neuronal dynamics with a delayed gain control model. PLoS Comput. Biol. *15*, e1007484.

48. Carandini, M., Heeger, D.J., and Movshon, J.A. (1997). Linearity and normalization in simple cells of the macaque primary visual cortex. J. Neurosci. *17*, 8621–8644.

49. Albrecht, D.G., Geisler, W.S., Frazor, R.A., and Crane, A.M. (2002). Visual cortex neurons of monkeys and cats: temporal dynamics of the contrast response function. J. Neurophysiol. *88*, 888–913.

50. Hollins, M., and Hudnell, K. (1980). Adaptation of the binocular rivalry mechanism. Invest. Ophthalmol. Vis. Sci. *19*, 1117–1120.

51. Brascamp, J.W., van Ee, R., Noest, A.J., Jacobs, R.H., and van den Berg, A.V. (2006). The time course of binocular rivalry reveals a fundamental role of noise. J. Vis. *6*, 1244–1256.

52. Rao, R.P.N., and Ballard, D.H. (1999). Predictive coding in the visual cortex: a functional interpretation of some extra-classical receptive-field effects. Nat. Neurosci. *2*, 79–87.

53. Sterzer, P., Kleinschmidt, A., and Rees, G. (2009). The neural bases of multistable perception. Trends Cogn. Sci. *13*, 310–318.

54. Lehky, S.R. (1988). An astable multivibrator model of binocular rivalry. Perception *17*, 215–228.

55. Shadlen, M.N., and Kiani, R. (2013). Decision making as a window on cognition. Neuron *80*, 791–806.

56. Wang, X.J. (2008). Decision making in recurrent neuronal circuits. Neuron *60*, 215–234.

57. Dijkstra, N., van de Nieuwenhuijzen, M.E., and van Gerven, M.A.J. (2016). The spatiotemporal dynamics of binocular rivalry: evidence for increased top-down flow prior to a perceptual switch. Neurosci. Conscious. *2016*, niw003.

58. Sterzer, P., Haynes, J.D., and Rees, G. (2006). Primary visual cortex activation on the path of apparent motion is mediated by feedback from hMT+/V5. Neuroimage *32*, 1308–1316.

59. Donner, T.H., Sagi, D., Bonneh, Y.S., and Heeger, D.J. (2013). Retinotopic patterns of correlated fluctuations in visual cortex reflect the dynamics of spontaneous perceptual suppression. J. Neurosci. *33*, 2188–2198.

60. Grassi, P.R., Schauer, G., and Dwarakanath, A. (2016). The role of the occipital cortex in resolving perceptual ambiguity. J. Neurosci. *36*, 10508–10509.

61. Vidal, J.R., Perrone-Bertolotti, M., Kahane, P., and Lachaux, J.P. (2015). Intracranial spectral amplitude dynamics of perceptual suppression in fronto-insular, occipito-temporal, and primary visual cortex. Front. Psychol. *5*, 1545.

62. van Kerkoerle, T., Self, M.W., Dagnino, B., Gariel-Mathis, M.A., Poort, J., van der Togt, C., and Roelfsema, P.R. (2014). Alpha and gamma oscillations characterize feedback and feedforward processing in monkey visual cortex. Proc. Natl. Acad. Sci. USA *111*, 14332–14341.

63. Wilke, M., Logothetis, N.K., and Leopold, D.A. (2006). Local field potential reflects perceptual suppression in monkey visual cortex. Proc. Natl. Acad. Sci. USA *103*, 17507–17512.

64. Buzsáki, G., and Draguhn, A. (2004). Neuronal oscillations in cortical networks. Science *304*, 1926–1929.

65. Kopell, N., Ermentrout, G.B., Whittington, M.A., and Traub, R.D. (2000). Gamma rhythms and beta rhythms have different synchronization properties. Proc. Natl. Acad. Sci. USA *97*, 1867–1872.

66. Tallon-Baudry, C., and Bertrand, O. (1999). Oscillatory gamma activity in humans and its role in object representation. Trends Cogn. Sci. *3*, 151–162.

67. Tallon-Baudry, C. (2009). The roles of gamma-band oscillatory synchrony in human visual cognition. Front. Biosci. *14*, 321–332.

68. Donner, T.H., and Siegel, M. (2011). A framework for local cortical oscillation patterns. Trends Cogn. Sci. *15*, 191–199.

69. Brascamp, J., Blake, R., and Knapen, T. (2015). Negligible fronto-parietal BOLD activity accompanying unreportable switches in bistable perception. Nat. Neurosci. *18*, 1672–1678.

70. Blake, R., Brascamp, J., and Heeger, D.J. (2014). Can binocular rivalry reveal neural correlates of consciousness? Philos. Trans. R. Soc. Lond. B Biol. Sci. *369*, 20130211.

71. Kelly, S.P., Lalor, E.C., Reilly, R.B., and Foxe, J.J. (2006). Increases in alpha oscillatory power reflect an active retinotopic mechanism for distracter suppression during sustained visuospatial attention. J. Neurophysiol. *95*, 3844–3851.

72. Doesburg, S.M., Bedo, N., and Ward, L.M. (2016). Top-down alpha oscillatory network interactions during visuospatial attention orienting. Neuroimage *132*, 512–519.

73. Engell, A.D., and McCarthy, G. (2010). Selective attention modulates face-specific induced gamma oscillations recorded from ventral occipitotemporal cortex. J. Neurosci. *30*, 8780–8786.

74. van Dam, L.C., and van Ee, R. (2005). The role of (micro)saccades and blinks in perceptual bi-stability from slant rivalry. Vision Res. *45*, 2417–2435.

75. Alais, D., and Melcher, D. (2007). Strength and coherence of binocular rivalry depends on shared stimulus complexity. Vision Res. *47*, 269–279.

76. Paradis, A.L., Cornilleau-Pérès, V., Droulez, J., Van De Moortele, P.F., Lobel, E., Berthoz, A., Le Bihan, D., and Poline, J.B. (2000). Visual perception of motion and 3-D structure from motion: an fMRI study. Cereb. Cortex *10*, 772–783.

77. Delorme, A., and Makeig, S. (2004). EEGLAB: an open source toolbox for analysis of single-trial EEG dynamics including independent component analysis. J. Neurosci. Methods *134*, 9–21.

78. Hermes, D., Miller, K.J., Noordmans, H.J., Vansteensel, M.J., and Ramsey, N.F. (2010). Automated electrocorticographic electrode localization on individually rendered brain surfaces. J. Neurosci. Methods *185*, 293–298.

79. Hoogenboom, N., Schoffelen, J.M., Oostenveld, R., Parkes, L.M., and Fries, P. (2006). Localizing human visual gamma-band activity in frequency, time and space. Neuroimage *29*, 764–773.

80. Siegel, M., Donner, T.H., Oostenveld, R., Fries, P., and Engel, A.K. (2007). High-frequency activity in human visual cortex is modulated by visual motion strength. Cereb. Cortex *17*, 732–741.

81. Benjamini, Y., and Hochberg, Y. (1995). Controlling the false discovery rate - a practical and powerful approach to multiple testing. J. R. Stat. Soc. Series B Stat. Methodol. *57*, 289–300.

82. Wang, L., Mruczek, R.E., Arcaro, M.J., and Kastner, S. (2015). Probabilistic maps of visual topography in human cortex. Cereb. Cortex *25*, 3911–3931.

Please cite this article in press as: de Jong et al., Intracranial Recordings Reveal Unique Shape and Timing of Responses in Human Visual Cortex during Illusory Visual Events, Current Biology (2020), https://doi.org/10.1016/j.cub.2020.05.082

STAR★METHODS

KEY RESOURCES TABLE

REAGENT or RESOURCE	SOURCE	IDENTIFIER
Software and Algorithms		
MATLAB (Mathworks)	http://www.mathworks.com/products/matlab/	RRID:SCR_001622
Analysis code	This paper; Open Sience Framework	https://osf.io/s45yb/
Presentation (Neurobehavioral Systems)	https://www.neurobs.com/	N/A

RESOURCE AVAILABILITY

Lead contact

Further information and requests for resources, data and code should be directed to and will be fulfilled by the Lead Contact, Maartje C. de Jong (m.dejong@spinozacentre.nl).

Materials availability

This study did not generate unique reagents.

Data and code availability

The analysis code and stimulus code generated during this study is available at the Open Science Framework (https://osf.io/s45yb/). The datasets supporting the current study have not been deposited in a public repository because of legal and ethical barriers to public archiving of patient data, but are available from the corresponding author on request after signing a data transfer agreement.

EXPERIMENTAL MODEL AND SUBJECT DETAILS

Participants

The present data are part of a larger dataset that was described previously [34]. The original dataset included an experiment with face-house binocular rivalry as well as an experiment with a rotating globe that was perceived rotating leftward or rightward (ambiguous structure-from-motion). Whereas percepts of faces and houses are known to be processed in anatomically segregated regions ([35, 36, 41, 42], face-house binocular rivalry [9], intracranial recordings in humans: [37–40]), different rotation directions are processed within the same motion-sensitive regions [14, 76]. Therefore, we re-analyzed only the data of the experiment with binocular rivalry for our investigation of percept-selective responses. The analysis included data of two participants with intractable epilepsy who underwent chronic subdural electrocorticography that included coverage of the occipital lobe for clinical reasons. Participant A was a 31 year old right-handed female with right-hemisphere electrode coverage. Participant B was a 28 year old left-handed male with right-hemisphere electrode coverage. Both participants had normal or corrected-to-normal vision and gave written informed consent before participation. The experiments were carried out at the University Medical Center Utrecht in accordance with the ethical guidelines in the Declaration of Helsinki (World Medical Association, 2000), after formal approval of the Medical Ethical Committee of the University Medical Center Utrecht (study number 07-260).

METHOD DETAILS

Illusory changes of the binocular rivalry stimulus

The stimuli, procedure and behavioral analysis are described in detail previously [34]. We also describe them briefly in the following four paragraphs. By means of red-green anaglyph glasses a house image was presented to the participant's left eye and a face image to their right eye (stereoscopic presentation; Figure 1A; images are courtesy of F. Tong [22]). The anaglyph glasses contained custom-made red and green filters. The participants reported no visible "cross talk" between the eyes. Due to the perceptual conflict between the eyes the participants alternatingly perceived the face or the house image (theory described in [21]). These spontaneously perceived changes are 'illusory', because the stimulus did not change. Both images subtended 2.9° horizontally and vertically. The small size and low contrast of the stimulus minimized the occurrence of mixture/piecemeal percepts (a face-house mixture) and produced relatively long-lasting percepts with a median duration of 4.1 (5.9) seconds and 4.6 (7.0) seconds for participants A and B, respectively (average durations in parentheses).

Physical changes of the stimulus

To compare illusory changes to actual, i.e., physical, changes to the stimulus, we alternatingly presented either the house-image (to the left eye) or the face image (to the right eye), while a uniform square was presented to the other eye (Figure 1B; all stimuli were the

Please cite this article in press as: de Jong et al., Intracranial Recordings Reveal Unique Shape and Timing of Responses in Human Visual Cortex during Illusory Visual Events, Current Biology (2020), https://doi.org/10.1016/j.cub.2020.05.082

same size as the binocular-rivalry stimulus). The participants always perceived the house/face image and not the uniform square. The median stimulus duration was 5.9 (10.0) seconds (average duration in parentheses; stimulus durations were based on percept durations during binocular rivalry reported by healthy volunteers in pilot tests). The replacements of the images elicited perceptual changes that were nearly indistinguishable in appearance to the illusory changes perceived with the binocular-rivalry stimulus. The important difference is that the stimulus physically changed, while the illusory changes occurred without a change in the stimulus (Figure 1). The participants were not informed about this difference.

Procedure

The participants sat in a semi-recumbent position in a hospital bed in a private room. Using Presentation (Neurobehavioral Systems) the stimuli were presented in the center of a computer screen (60 Hz refresh rate) that was positioned in front of the participant at a viewing distance of 85 cm. Throughout the experiment a constant binocular pattern of lines that extended 15.8° horizontally and vertically into the periphery surrounded the stimuli to facilitate proper alignment of the eyes. The participants were instructed to fixate the center of the house/face image and report every perceptual change that they experienced by pressing one of two corresponding buttons on a button box held in the preferred hand (both used the right hand). They were also instructed to stop the experiment when the 'target'-percepts, i.e., the house or the face, did not predominate. However, both participants reported clear percepts without discernable piecemeal percepts (in line with pilot tests on healthy volunteers). Both participants completed two experimental sessions that each consisted of four 2-minute blocks of stimulation interleaved with 10 s of rest. The blocks of stimulation alternatingly contained either the binocular-rivalry stimulus or the stimulus with physical changes.

Electrocorticographic recording and processing

The subchronic electro-corticographic recordings were part of a presurgical assessment to localize the epileptic focus for surgical removal. Continuous recording from subdural electrodes (2.3 mm exposed diameter, interelectrode distance 1 cm; Ad-Tech Medical Instrument) was done using a 128-channel Micromed system (22 bits; bandpass filter, 0.15–134.4 Hz) and a sampling frequency of 512 Hz. The recorded data were analyzed using in-house-developed MATLAB code and the open source MATLAB tool-box EEGlab ([77]; MATLAB, MathWorks Inc.; in-house developed code available at Open Science Framework: https://osf.io/s45yb/). The recordings were visually inspected for epileptiform activity, artifacts and technical failure, leading to exclusion of one anterior temporal grid in participant A and one anterior temporal electrode of participant B (Figures 2A and 2B). The remaining electrode signals were referenced to their common average and analyzed further, with the exception of electrodes placed on top of another grid and electrodes covering somatosensory or motor cortex (as identified by comprehensive clinical testing and anatomical landmarks; Figures 2A and 2B). The latter were excluded because motor and sensory processing related to pressing the response button were not of interest in the present study. The location of the electrodes was determined using a pre-operative anatomical magnetic resonance imaging (MRI) scan that was co-registered to a computed tomography (CT) scan made after implantation, following the method described in [78].

From the continuous data we extracted epochs time-locked to reports, i.e., button presses that indicated the participant perceived a physical or illusory change, as well as epochs time-locked to physical stimulus changes, i.e., the timing of on-screen changes. A time–frequency transformation with frequency steps of 1 Hz and time steps of 50 ms was applied over the 50–130 Hz frequency band of interest (following [34] and previous literature on physical changes [4, 43, 63, 66–68, 79, 80]:). A 75.9–97.5 cycle Morlet wavelet was used for the frequency range of 50-130 Hz, respectively, which was tapered with Hanning window. To normalize power scaling across frequencies (i.e., higher frequencies having smaller raw power values [64]), power was normalized per epoch, per frequency, by dividing power by the mean power over a 5 s wide time-window centered on the event. Then, a baseline correction was applied by subtracting the mean power in a 500-ms time-window that directly preceded the time-window in which event-related power changes were expected. Regarding reports, event-related activity was expected to emerge from −1500 ms before the report onward [13, 34], so the baseline interval spanned −2000 to −1500 ms prior to the report. Regarding on-screen changes, we were interested in the response elicited directly after the on-screen change, so the baseline interval spanned −500 to 0 ms prior to this change. Power was then averaged across the frequency band of interest.

QUANTIFICATION AND STATISTICAL ANALYSIS

Behavioral analysis

We excluded the very first report of each block, because this reflected perceived onset of the stimulus rather than a perceptual change from face to house or vice versa. When the same report was given twice consecutively, we excluded the second report (this occurred 3 times for reports of illusory changes by participant A). Additionally, when reports followed each other within 1000 ms, we excluded the second report because its epoch could be contaminated by neural activations associated with the earlier report (this occurred 2 times for reports of illusory changes by participant B). For physical changes we used additional exclusion criteria (excluding incorrect reports and reaction times > 3500 ms), but none of the reports was excluded based on these criteria. Median reaction times were 829 (830) ms and 627 (741) ms for participant A and participant B, respectively (mean reaction times in parentheses).

Please cite this article in press as: de Jong et al., Intracranial Recordings Reveal Unique Shape and Timing of Responses in Human Visual Cortex during Illusory Visual Events, Current Biology (2020), https://doi.org/10.1016/j.cub.2020.05.082

Identification and tuning of electrodes

For each electrode and each of the 4 conditions (physical/illusory; house-/face onset) we calculated the peak amplitude in high-frequency power (50-130 Hz) occurring −1000 to 0 ms relative to the report, reasoning that the perceptual change occurred before the participant reported it (used time-window follows [13, 34] but is narrower because we needed to capture the peak rather than the entire course of the response). Peaks falling on the edge of the time-window were only included if they reflected true peaks and excluded from the analysis if the amplitude increased further outside the time-window (89.9% of epochs included across electrodes). Per electrode we then performed a two-way analysis of variance (ANOVA) with *type-of-change* (physical/illusory change) and *perception* (house-/face onset) as between factors, controlling false discovery rate using the Benjamini-Hochberg procedure [81] (using MATLAB, MathWorks Inc.). We selected all electrodes with a significant main effect and/or interaction. We chose a selection procedure based on peak amplitude of the responses, because it is independent of our measures of interest (response shape and timing). We did not use a time-window relative to the stimulus change for physical changes (as we do below in the analysis of response timing), because the within-electrode comparison between physical and illusory changes we do here requires using the same method for both types of changes.

Location of electrodes

In both participants there was a lateral and a ventral cluster of selected electrodes, located superior and inferior to the occipito-temporal sulcus, respectively. Within these clusters we used the imaginary line between the pre-occipital notch and the parieto-occipital sulcus to estimate whether electrodes were covering the occipital or temporal lobe [34]. We applied an automated segmentation algorithm that uses anatomical landmarks to estimate the locations of primary visual cortex (V1), secondary visual cortex (V2) and motion-selective mediotemporal region (V5/MT; Freesurfer Software Suite; http://surfer.nmr.mgh.harvard.edu). In addition, in certain cases we consulted probabilistic maps of visual cortex described in [82]. Note that all estimations of functional regions were based on anatomical landmarks and were not verified by functional mapping experiments. Although this method supports coarse estimation, it does not allow very specific or definite functional localization (e.g., individual variability and effects of volume condition are not considered). Localization precision was also limited by the quality of the anatomical MRI scans and the co-registration with the post-implantation CT scan.

The lateral electrodes were classified as covering lateral extrastriate visual cortex, because none of these electrodes covered estimated V1. Electrodes classified as covering occipital cortex were a3, a4, b2 and b3 in participant A and a2, a3, b1, b3, b4, b5, b6, b7 in participant B. A subset of the occipital electrodes covered estimated V2 (a3, b2 and b3 in participant A; b1 and a2 in participant B; Freesurfer also assigned ventral electrode c2 in participant B to V2). Electrode a4 in participant A was estimated to cover visual area 3 (V3; following [82]). Electrodes b6 in participant A and b5 and b7 in participant B were estimated to cover V5/MT. Electrodes classified as covering temporal cortex were b6, a7, a9 and a10 in participant A (the latter three being close to the superior temporal sulcus) and a7 in participant B.

The ventral electrodes were classified as covering ventral occipito-temporal cortex, including lingual gyrus and posterior fusiform/parahippocampal gyrus. Although we were unable to reliably localize the collateral sulcus which separates the fusiform and parahippocampal gyrus, the localization of the ventral electrodes and their tendency to have a strong perception preference suggests they may cover the fusiform face area [42] or the parahippocampal place area [36]. In participant A, electrodes c2, c3, c4 and c5 were classified as covering occipital cortex (possibly lingual gyrus or occipital portion of fusiform gyrus), while c6 covered temporal cortex (most likely fusiform gyrus). In participant B the ventral electrodes were all classified as covering temporal cortex (likely covering fusiform/parahippocampal gyrus but not lingual gyrus) and, relative to c6 in participant A, they were located slightly more anterior.

The shape of responses

To assess the shape of the responses we calculated the best fit of a skewed Gaussian to the single-epoch data. We used a skewed function, because neural responses are often skewed to the right (fast rise, slow decay). Moreover, it has been suggested that neural responses associated with illusory changes instead have a relatively slow rise [13, 46], which would result in a skew to the left (although these suggestions were based on averaged epochs aligned to the report and may thus reflect differences in reaction times in addition to differences in neural responses, as shown in Figures S1 and S3B). The following function was used: power = amplitude * e^G * (1+erf(skew*t)), where t = (time-timeshift)/duration, e^G refers to the Gaussian function (G = $-t^2$; *e* is a mathematical constant known as Euler's number) and erf refers to the Gauss error function. The procedure was performed on a −750 to +750 ms time-interval spanning the peak of the single-epoch response (we used the peaks obtained in the electrode section procedure described above). We analyzed the amplitude, skew and duration parameters (the timeshift parameter mostly reflected shifts in the peak of the fit due to nonzero skew and was therefore not analyzed). By taking the peak of the response as the starting-point for the fit procedure, we ignored the delay between the neural activation and the report and eliminated any influence of reaction time (see Figures S1 and S3B for assessment of the influence of reaction times). Fits for which $r < 0.1$ were excluded from the analysis (14% of epochs were excluded; repeating the analysis without excluding these epochs yielded equivalent results). All analyses were performed using MATLAB (MathWorks Inc.; in-house developed code available at Open Science Framework: https://osf.io/s45yb/) and statistical details are provided in the Results section (significance was defined at $p < 0.05$).

Please cite this article in press as: de Jong et al., Intracranial Recordings Reveal Unique Shape and Timing of Responses in Human Visual Cortex during Illusory Visual Events, Current Biology (2020), https://doi.org/10.1016/j.cub.2020.05.082

The timing of responses

For all electrodes that responded to perceptual changes (Figures 2A and 2B) we determined the peak latency of the high-frequency responses in the conditions that the electrode's responses were tuned to. Since reaction times are thought to be relatively slow and variable for illusory compared with physical changes [27–29] and may also differ between house and face reports (Figure S1A), we wanted to bypass any influence of reaction times in our analyses. Therefore, we were not interested in the absolute latencies (delay to report), but instead compared latencies between electrodes. We performed this analysis for each possible pair of electrodes with responses tuned to the same percept in the same participant (Figure 4). For all analyses, we excluded epochs for which the peak of one or both electrodes fell on the edge of the used time-window in case the amplitude increased further outside the time-window, i.e., peaks on the edge of the time-window were only included if they reflected true peaks. Analysis was done per electrode-pair, because including more electrodes in a comparison could lead to more epochs being excluded. For the comparison including electrode d10 in participant B we additionally excluded epochs with small power change ($< 0.35\ \mu V^2$ in 500-ms time-window centered on epoch-specific averaged peak latency; this applied to 17% of epochs), because the rounded shape and low amplitude of this electrode's response to illusory changes otherwise compromised reliable determination of peak latency (Figure 4F, graph on the right; Figure S1C, graph on the lower right). Across participants and electrode-pairs the average number of included epochs was 14.5 (68%) and 28.2 (74%) for physical and illusory changes, respectively.

Regarding illusory changes we adopted a coarse-to-fine method in which we first determined peak latencies relative to the report and averaged these across both electrodes in a pair. This averaged peak latency provided a reference time-point that subsequently guided more precise determination of differences in peak latency between individual electrodes. We verified and adjusted the time-window used to determine peak latencies relative to the report, based on observations of each participant's reaction times and the selected electrodes' averaged responses aligned to the report (examples in Figure S1). For participants A and B the used time-windows spanned −1000 to +100 ms and −1000 to −100 ms relative to the report, respectively. The window for participant A spanned until +100 ms, because some averaged responses peaked around the moment of the report and we wanted to preclude single-epoch latencies falling on the upper edge of the window for these responses (example in Figure S1C, top right graph). The window for participant B was 200 ms smaller, because some responses showed two consecutive peaks and we wanted to capture the earliest peak (example in Figure S1C, bottom right graph). Also, this narrower window gains precision and acknowledges that the median reaction time was about 200 ms longer in this participant (829 for participant B versus 627 ms for participant A). For comparisons including electrode c4 in participant A we adjusted the lower edge of the window (to −750 ms) in order to exclude the earliest of two consecutive peaks present in the response of c4 (Figure S1B, top graph). Note that the selection of the time-window did not influence the comparison between electrodes, as we always used the same window for both electrodes in a pair. Peak latencies relative to the report were averaged per electrode-pair, per epoch, and used as a reference time-point to precisely determine peak latencies in individual electrodes. For each of the two electrodes in a pair we then determined, per epoch, the maximum amplitude in a 500-ms wide time-window centered on the reference time-point.

Regarding physical changes there was no need to use this coarse-to-fine method, as the timing of the on-screen stimulus change provided a precise reference time-point shortly after which the perceptual change should occur. Therefore, we determined peak latencies for physical changes over a +100 to +450 ms time-window after the stimulus change and then calculated the per-epoch differences for each electrode-pair. In addition to the relative latencies presented in Figure 4, we show absolute latencies for physical changes in Figure 5. All analyses were performed using MATLAB (MathWorks Inc.; in-house developed code available at Open Science Framework: https://osf.io/s45yb/) and statistical details are provided in the Results section (significance was defined at $p < 0.05$).

Current Biology, Volume *30*

Supplemental Information

Intracranial Recordings Reveal Unique Shape and Timing of Responses in Human Visual Cortex during Illusory Visual Events

Maartje C. de Jong, Mariska J. Vansteensel, Raymond van Ee, Frans S.S. Leijten, Nick F. Ramsey, H. Chris Dijkerman, Serge O. Dumoulin, and Tomas Knapen

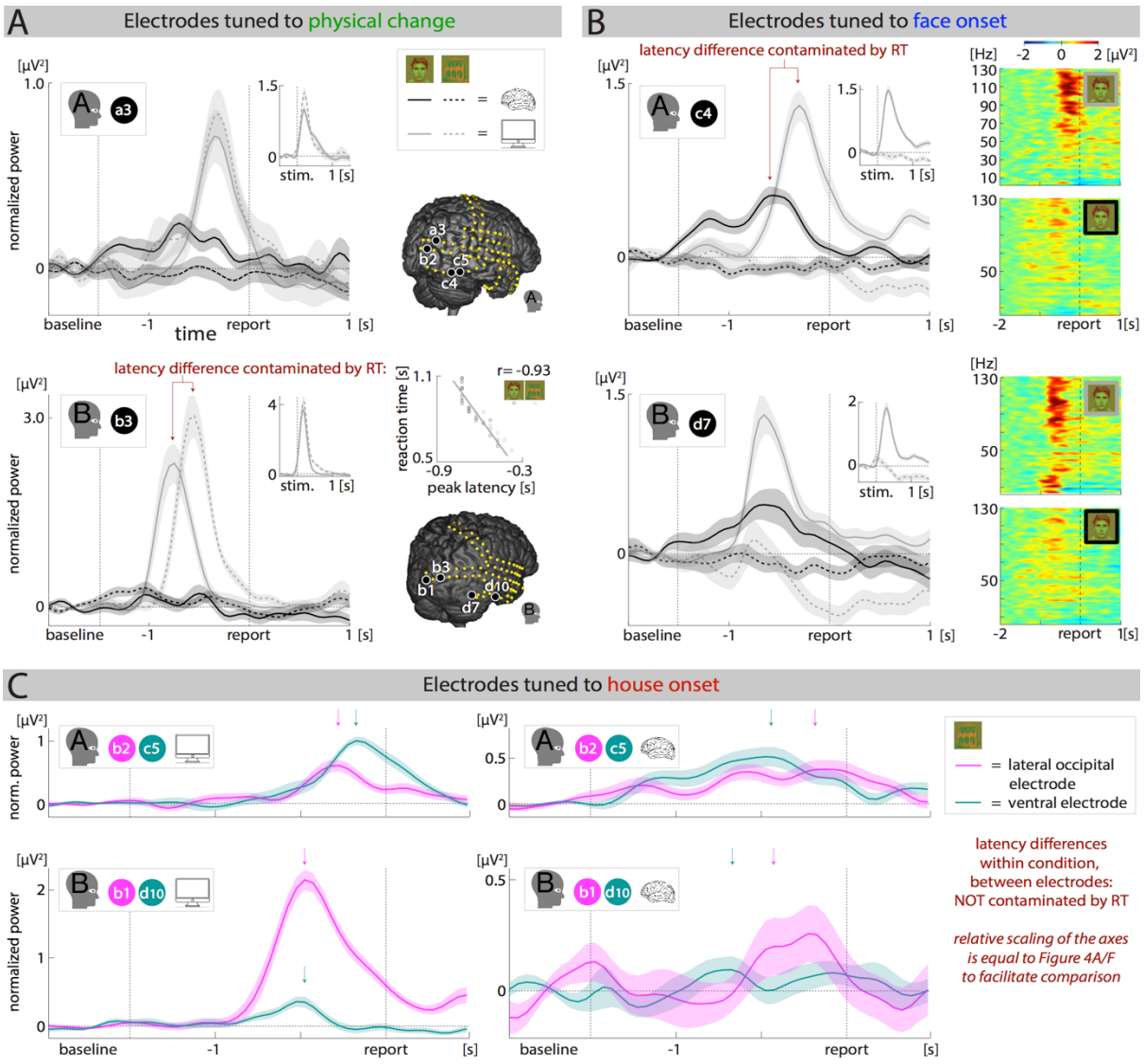

Figure S1: Tuning of electrodes is evident from averaged responses that are aligned to the report, but response shape and timing of these averages are contaminated by reaction times. Related to Figures 2, 3 and 4 .

(A) Responses aligned in time to the report (indicated by 'report' on the horizontal axis), recorded from lateral occipital electrodes tuned to physical changes in participant A (top graph; electrode a3) and participant B (bottom graph; electrode b3). These electrodes activated to physical changes only, regardless of the content of perception. Solid and dashed lines indicate face and house onsets, respectively. Black and grey lines indicate illusory and physical changes, respectively. As these averaged epochs were aligned to the moment of the report, they reflect neural factors as well as the magnitude and variability of reaction times ('RT'). For example, the response to physical face onsets precedes the response to physical house onsets in participant B but not in participant A, likely because reaction times were faster for house than for face onsets in participant B ($t_{(40)}$= 3.4, p= 0.001) but not participant A ($t_{(40)}$= 0.6, p= 0.5). The scatter plot for electrode b3 in participant B shows the strong relation between peak latency and reaction time. Insets: same epochs elicited by physical changes, now aligned in time to the on-screen change in the stimulus (the latency difference in participant B is absent here, confirming that it reflected a difference in reaction times). Brain maps: location of electrodes presented in panels A-C. Shading indicates ±SEM (across epochs).

(B) Responses aligned in time to the report recorded from posterior fusiform electrodes tuned to face onsets in participant A (top graph; electrode c4) and participant B (lower graph; electrode c7). These electrodes activated to onset of the face percept (solid lines) and not the house percept (dashed lines), regardless of whether the change was physical or illusory. Conventions as in panel A. On the right of each graph: corresponding time-frequency spectra for physical (top) and illusory (bottom) face onsets. Since these responses were aligned to the report and then averaged, any difference between illusory and physical changes regarding response latency or response shape could reflect a difference in reaction times. Reaction times are thought to be longer and more variable for illusory compared with physical changes [27-29]. When responses are aligned to the report, such a difference in reaction times will be reflected in averaged responses with a lower amplitude, longer duration and earlier timing for illusory compared with physical changes (i.e., differences between illusory and physical changes will be exaggerated, see analysis in Figure S3B; compare with responses aligned to peak in Figure 3C). Importantly, all analyses described in the main text were performed at the single-epoch level to eliminate any influence of reaction times.

(C) Responses aligned in time to the report recorded from a lateral occipital electrodes (pink) and ventral electrodes (cyan) tuned to house onsets in participant A (top) and participant B (bottom). In Figures 4A and 4F the same data are presented (there epochs were aligned in time to averaged peak latency). Here, epochs are aligned to the report to illustrate the influence of reaction times. Conventions and relative scaling of vertical and horizontal axis are adopted from Figures 4A and 4F to facilitate comparison (physical house onsets on the left; illusory house onsets on the right; responses to face onsets not shown). Possible differences in reaction times prohibit direct comparison of response shape and latency between illusory and physical changes, but do not affect within-condition comparison of latencies between electrodes. Therefore, the differences in response latency presented in Figure 4 are also seen here: regarding physical changes lateral occipital responses either precede ventral responses or occur at similar latency, whereas lateral occipital responses are later than ventral responses regarding illusory changes.

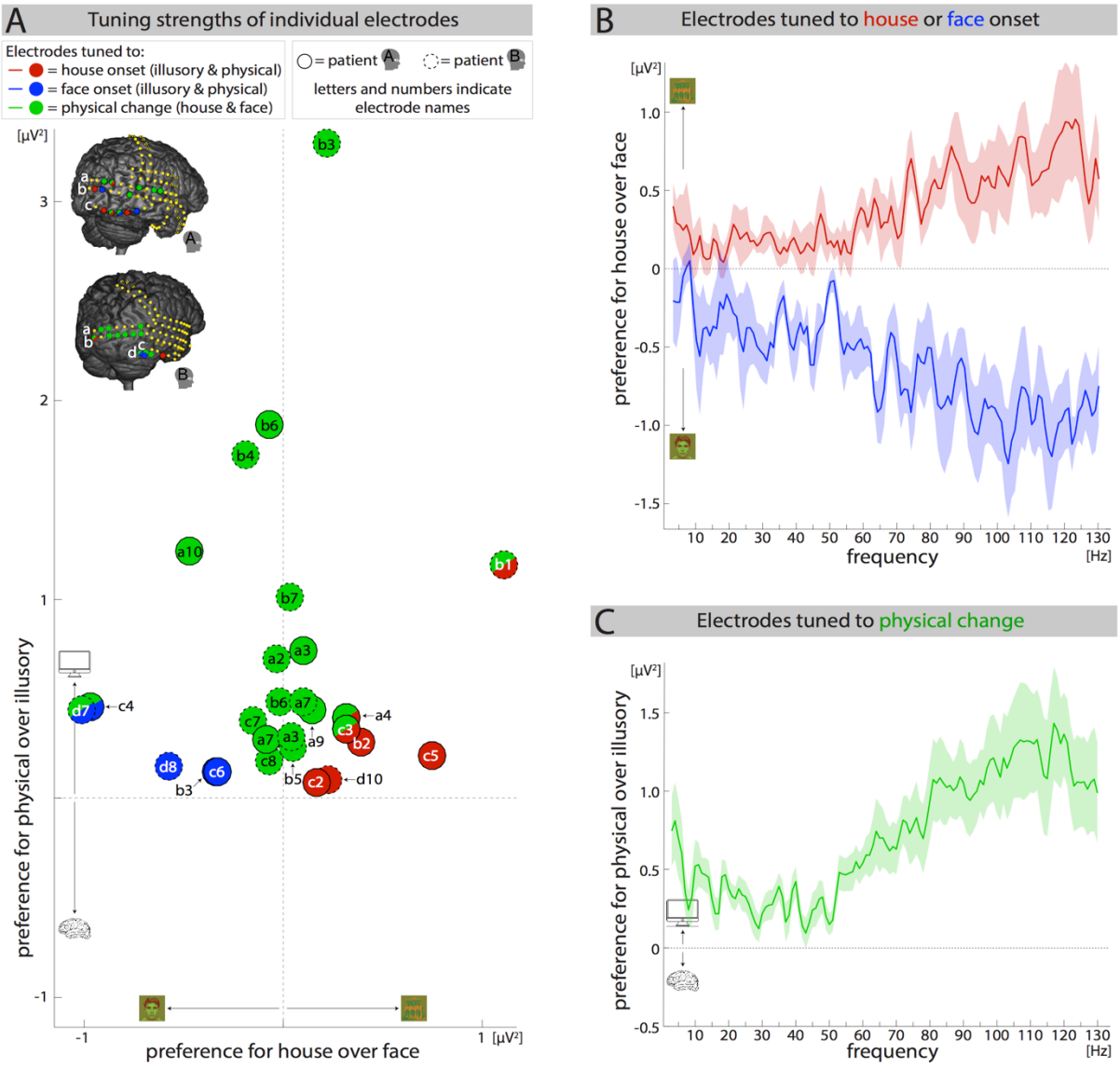

Figure S2: Tuning strengths for individual electrodes (panel A) and individual frequencies (panels B-C). Related to Figure 2.

(A) Tuning strengths of individual electrodes that responded to perceptual changes (in 50-130 Hz frequency range). Horizontal axis: preference for onset of the house percept over the face percept, i.e., average difference in power change between the two possible percepts (defined as: (Hp+Hi)/2 - (Fp+Fi)/2, where 'H' refers to house onsets, 'F' to face onsets, 'p' to physical changes and 'i' to illusory changes). Vertical axis: preference for physical changes over illusory changes, i.e., response to physical changes minus response to illusory changes (defined as: (Hp+Fp)/2 - (Hi+Fi)/2). Electrodes near the cardinal axes were either perception-tuned (blue or red) or tuned to physical changes (green). Five electrodes showed a combination of both tuning patterns (half-green, half-red/blue). For two out of these five electrodes a significant interaction indicated that perception preference was stronger when the change was physical (c4 in participant A; b1 in participant B). Conventions as in Figure 2. Regarding electrodes without responses tuned to certain perceptual changes (electrode depicted as bright yellow circles without X-mark in Figure 2A-B), an additional analysis indicated that all but one of these electrodes exhibited no responses to perceptual changes at all. For this additional analysis we compared maximum amplitude in the time-window of interest to a

reference time-window (time-windows: -1000 to 0 ms and +1000 to +2000 ms relative to the report, respectively; factor *time-window* was added to ANOVA described in STAR Methods under subheading 'Identification and tuning of electrodes'). One electrode in the parietal electrode grid in participant B responded to all perceptual changes (electrode on the left in the third row from above, see electrode layout in Figure 2B). Considering this electrode covered the postcentral sulcus, these responses likely reflect the manual report of the participant.

(B) Tuning strength of electrodes tuned to house (red) and face (blue) onsets for single frequencies between 3-130 Hz. Tuning to perception is evident in high- but not low-frequency power changes. Data are averaged across participants and electrodes, i.e., across the 12 electrodes that are (half-)red/blue in panel A. Considering previous literature describing decreases in alpha power [4, 34, 61-63] (see Discussion), we analyzed the latency of the minimum alpha power for these electrodes (equivalent to analysis in Figure 4, but here for the 8-13 Hz frequency band). These latencies neither showed differences between electrodes, nor any reversal of latency differences when comparing physical and illusory changes. We also assessed whether perception-tuned responses in the alpha range were present on other electrodes (equivalent to analysis in Figure 2, but for the 8-13 Hz frequency band). In neither participant we found such responses. Shading indicates ±SEM (across electrodes).

(C) Tuning to physical changes is evident in broadband high-frequency power changes. Tuning strengths of electrodes tuned to physical changes (green electrodes in panel A) for single frequencies between 3-130 Hz. Data are averaged across electrodes and participants. Shading indicates ±SEM (across electrodes).

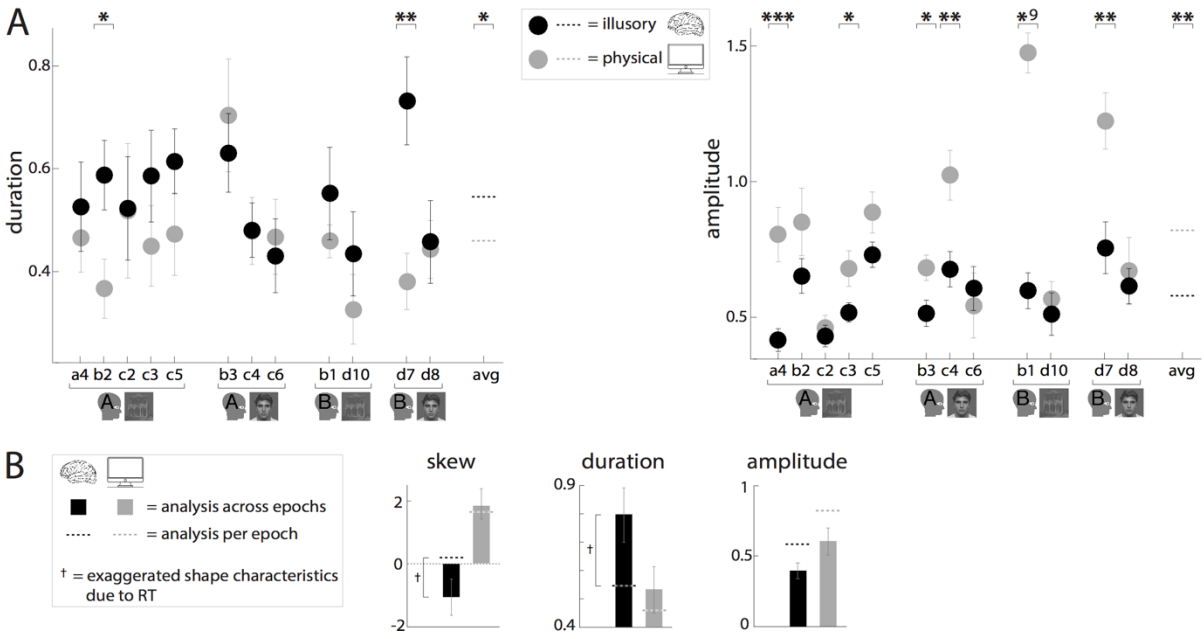

Figure S3: Differences in response shape between illusory and physical changes are consistent across electrodes (panel A) and appear exaggerated when epochs aligned to the report were analyzed (panel B). Related to Figure 3.

(A) The duration (left) and amplitude (right) of the skewed Gaussians fitted to illusory (black) and physical (grey) onsets of the preferred percept for each of the perception-tuned electrodes (response skew is presented in figure 3D). The analysis was performed per epoch (as in Figure 3). Horizontal dashed lines represent averages across electrodes as presented in Figure 3E. Asterisks reflect the difference between physical and illusory changes: * indicates $p< 0.05$, ** indicates $p< 0.01$, *** indicates $p< 0.001$, $*^{9}$ indicates $p< 0.000000001$. Error bars indicate ±SEM (across epochs).

(B) The influence of reaction times on the shape of averaged responses aligned to the report is analyzed here by performing the shape analysis on all epochs at ones (aligned to the report; black bars: illusory changes; grey bars: physical changes). Horizontal dashed lines represent results of the original single-epoch analysis (Figure 3; epochs removed in the single-epoch analysis were also removed in the analysis across epochs). In comparison with the single-epoch analysis, fitted responses for illusory changes were longer-lasting and had a more negative skew (difference between analyses, duration: $t_{(11)}= 2.4$, $p= 0.04$; skew: $t_{(11)}= 2.1$, $p= 0.06$). For physical changes duration and skew did not differ between the analyses (both $t_{(11)}< 0.9$, both $p\geq 0.4$). The differences in response-shape between illusory and physical changes were thus exaggerated in the analysis across epochs, indicative of a relatively wide and rightward-skewed reaction time distribution for illusory compared with physical changes. The amplitude of the fitted responses was lower in the analysis across epochs than in the analysis per epoch (illusory and physical changes: both $t_{(11)}> 5.1$, both $p\leq 0.0003$). Error bars indicate ±SEM (across electrodes).